Studies on novel physiological activities of *Citrus sudachi* peel extract and its components

Shogo Abe

Department of Biological Science and Technology,
Graduate School of Advanced Technology and Science and of
Biological Science and Technology
Tokushima University

March 2022

CONTENTS

Abbreviation

ANOVA	analysis of variance
BG	1,3-butylene glycol
Bid	BH3-interacting domain death agonist
BrdU	5-bromo-2’-deoxyuridine
cSCC	cutaneous squamous cell carcinoma
DMEM	Dulbecco’s modified Eagle’s medium
DMSO	dimethyl sulfoxide
EGF	epidermal growth factor
EGFR	epidermal growth factor receptor
Elk-1	ETS domain-containing protein
ERK1/2	extracellular signal-regulated kinase 1/2
FBS	fetal bovine serum
GAPDH	glyceraldehyde 3-phosphate dehydrogenase
HaCaT	human adult low-calcium high-temperature
HPLC	high performance liquid chromatography
JNK	Jun amino terminal kinase
LC3	microtubule-associated protein light chain 3
LDH	lactate dehydrogenase
MAPK	mitogen-activated protein kinase
MEK1/2	MAPK/ERK kinase 1/2
MKK3/6	MAP kinase 3/6
MTT	3-(4,5-dimethyl-2-thiazolyl)-2,5-diphenylte-trazolium bromide
NHEK	normal human epidermal keratinocytes
PARP	poly (ADP-ribose) polymerases
PBS	phosphate buffered saline
PI	propidium iodide
PMF	polymethoxyflavone
ROS	reactive oxygen species
RT-PCR	real-time polymerase chain reaction
SE	standard error
SPE	*Citrus sudachi* peel extract
TGF	transforming growth factor
TNF	tumor necrosis factor
z-VAD-FMK	N-benzyloxycarbonyl-Val-Ala-Asp(O-Me) fluoromethyl ketone

Chapter 1 General introduction

1. Skin

The skin is a barrier that separates the body from the external environment and plays essential roles in regulating water loss and protecting the body from ultraviolet radiation and microbial infection [1]. The skin comprises three layers: the epidermis, dermis, and subcutaneous layer. The outermost epidermis is mostly composed of keratinocytes (~90%). Exposure to UV radiation results in DNA damage, which causes mutations; this is considered as an event initiating skin carcinogenesis. The elimination of UV radiation-damaged keratinocytes via apoptosis is an essential mechanism for protecting the skin from sunlight. However, the increased proliferative and reduced apoptotic abilities of keratinocytes causes abnormal proliferation, leading to conditions such as skin cancer, psoriasis, keratosis, verrucae, and lichen simplex chronicus [2].

The outermost epidermis is composed of a stratified epithelium with distinct layers of keratinocytes [3]. Keratinocytes differentiate sequentially from the stratum basale to the stratum spinosum, stratum granulosum, stratum lucidum, and stratum corneum. During differentiation, keratinocytes express specific genes in distinct layers of the epidermis. For example, the expression of keratin 1 and keratin 10 is promoted in the stratum spinosum (early differentiation markers), whereas that of filaggrin is primarily detected in the stratum granulosum [4]. A continuous steady state of proliferation and differentiation of keratinocytes results in the constant renewal of the epidermis, providing an effective barrier for the skin. Disruption of this balance between proliferation and differentiation in keratinocytes leads to skin disorders, such as psoriasis, atopic dermatitis, and ichthyosis vulgaris [4, 5].

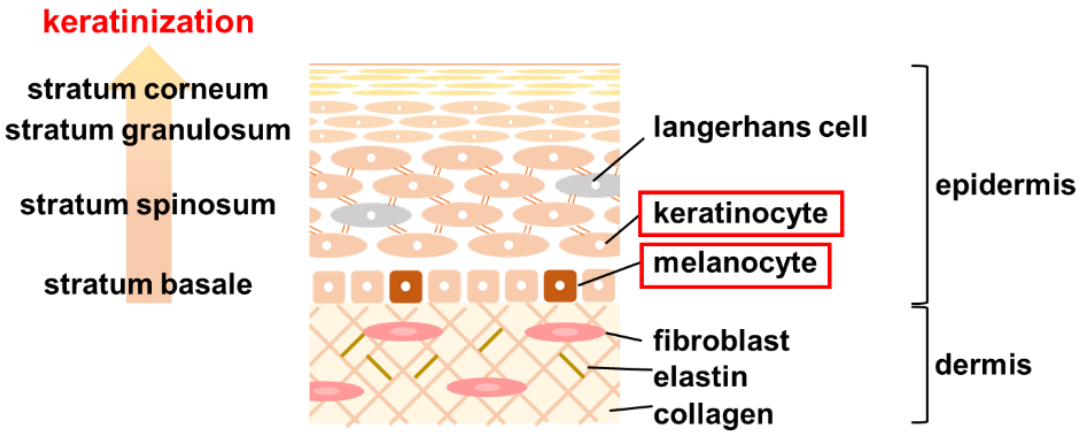

Figure 1. Skin structure.

2. Cell death

In multicellular organisms, cell death is an important process that maintains tissue homeostasis and eliminates potentially harmful cells [6]. There are various modalities of cell death, including apoptosis (type I), autophagic cell death (type II), and necrosis (type III) [7]. Apoptosis and autophagic cell death are not completely distinct and are affected by each other [8]. Apoptosis usually functions to maintain homeostasis in cell populations in development and aging [9]. It induces morphological changes, such as cell shrinkage, membrane blebbing, chromatin condensation, and nuclear fragmentation, which are almost triggered by activation of the caspase family of cysteine proteases. Apoptosis also plays a pivotal role in eliminating genetically damaged cells that might progress to cancer. Therefore, there have been many trials to develop new compounds that induce apoptosis.

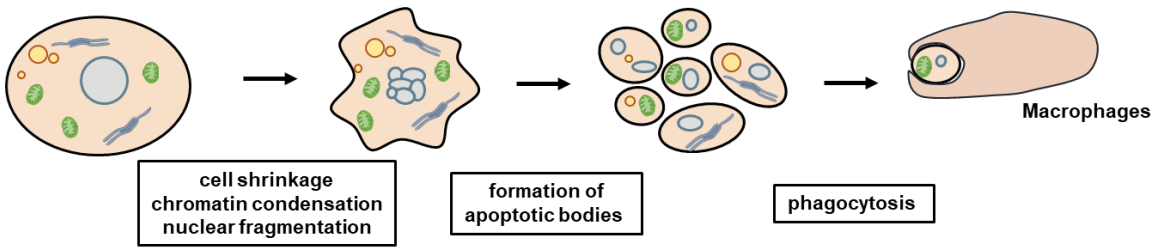

Figure 2. apoptosis process.

On the other hand, autophagy constitutively occurs at low levels to degrade cytoplasmic components including damaged organelles and long-lived proteins, but it is dramatically induced by stresses, such as nutrient starvation and oxidative stress, to promote cell survival [10, 11]. It begins with the formation of autophagosomes, followed by their fusion with lysosomes to produce autolysosomes where the engulfed content is digested by lysosomal hydrolases. Although the overactivation of autophagy may result in autophagic cell death, autophagy dysfunction is associated with a number of diseases, including infection, cancer, and neurodegeneration, suggesting that targeting autophagy may be an attractive therapeutic approach.

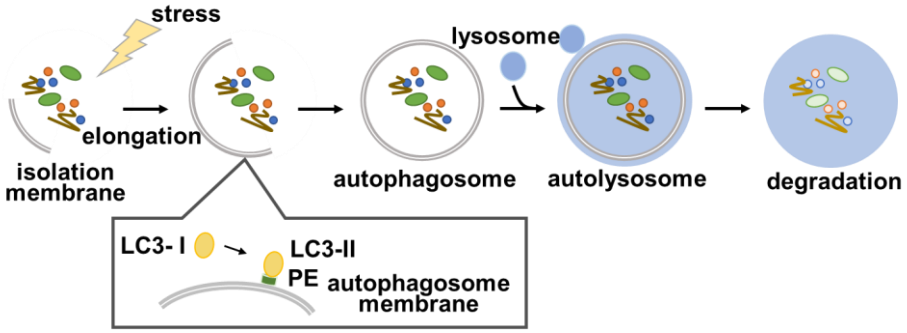

Figure 3. autophagy process.

3. *Citrus sudachi* and its functional components

Citrus sudachi is mainly produced in Tokushima Prefecture, Japan, and is included in the flavorful acid citrus fruit group. Around half of the total production of *C. sudachi* is consumed as fresh fruit, and the other half is consumed as processed products, such as juices. The citrus peel waste of the juice extraction process contains phytochemicals such as vitamins, minerals, flavonoids, coumarin, limonoids, carotenoids, and pectin, which possess a variety of biological functions including antioxidant, anti-inflammatory, antimutagenic, anticarcinogenic, and anti-aging properties [12]. For example, anthocyanins found in typical Italian pigmented orange (*Moro*, *Tarocco* and *Sanguinello*), have a high antioxidant activity. It has also been reported that flavonoids such as nobiletin and tangeretin including in citrus peel have antiallergic, anticancer antioxidant

and anti-inflammatory properties. In addition, many reports show that citrus peel extract has beneficial bioactivity (e.g., *Citrus sinensis* peel extract shows anti-aging activity by downregulation of MMP1 expression, and *Citrus nobilis* peel extract has antioxidant, antimicrobial, and anti-inflammatory activity [13, 14]). Therefore, the citrus peel has potential for use in the food, cosmetic, and pharmaceutical industries. Since the peel of *C. sudachi* also contains many phenolic compounds, such as hesperidin, naringin, narirutin, and sudachitin, which have anti-inflammatory and antioxidant properties [15, 16], it is expected that the extract of *C. sudachi* peel has various beneficial physiological properties. Recently, although it was reported that the extracts of *C. sudachi* peel attenuate body weight gain in mice fed a high-fat diet and improve lipid metabolism, its other biological activities are not yet fully understood [17, 18]

Flavonoids are polyphenolic compounds and bear a phenyl benzopyrone structure, representing as two benzene rings joined by a linear three-carbon chain, with a carbonyl group at the C-4 position [19]. The citrus flavonoids are divided into a class of glycosides (e.g., hesperidin and naringin) and polymethoxyflavones (PMFs), a class of methylated aglycones of flavones, (e.g., nobiletin and tangeretin). PMFs are almost exclusively found in the peel of citrus fruits, also possess various biological activities such as anti-cancer, anti-inflammation, and anti-atherosclerosis as well as neuroprotective effects [19, 20, 21]. For example, nobiletin (5,6,7,8,3',4'-hexamethoxyflavone) (Figure 4, right), which is a typical PMF from the peel of *Citrus depressa* and is one of the most studied flavonoids, exhibits anti-inflammatory and carcinogenesis-inhibitory activities [22, 23]. Moreover, tangeretin (5,6,7,8,4'-pentamethoxy-flavone) is also a polymethoxylated flavone present in the peel of citrus fruits has antiproliferative and anticarcinogenic effects [24]. Other PMFs, sudachitin (5,7,4'-trihydroxy-6,8,3'-trimethoxy-flavone) (Figure 4 left) and 3'-demethoxy-sudachitin (5,7,4'-trihydroxy-6,8-dimethoxyflavone) (Figure 4, middle), have been isolated from the peel of *C. sudachi*, a well-known fruit in Tokushima Prefecture, Japan [25]. It has been reported that sudachitin exhibit several biological activities. For

examples, sudachitin possesses an anti-inflammatory property in LPS-stimulated macrophages by suppressing the expression of inducible nitric oxide synthase, and blocks LPS-induced inflammatory bone destruction by directly inhibiting osteoclast differentiation from osteoclast precursors [26, 27]. In addition, previous study showed that sudachitin suppresses matrix metalloproteinase-1 and matrix metalloproteinase-3 production in TNF-α-stimulated human periodontal ligament cells by inhibiting the Akt pathway [28]. Moreover, sudachitin reduces gain of body weight in mice fed a high fat diet by enhancing energy expenditure through regulation of sirtuin1, peroxisome proliferative-activated receptor gamma coactivator-1-α and uncoupling protein-1 gene expression levels [29]. Sudachitin also enhances antigen-specific cellular and humoral immune responses in BALB/c mice [29]. However, its biological activities are not yet investigated in skin.

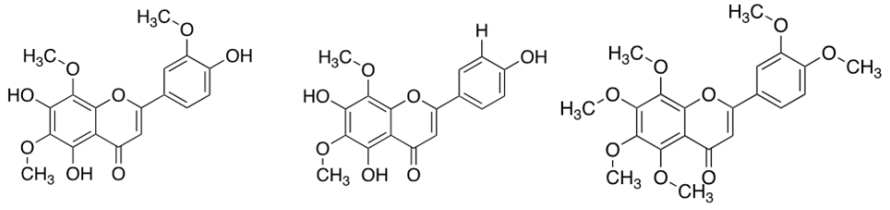

Figure 4. Chemical structure of PMFs.

Chemical structure of sudachitin (5,7,4'-trihydroxy-6,8,3'-trimethoxyflavone), 3'-demethoxysudachitin (5,7,4'-trihydroxy-6,8-dimethoxyflavone), and nobiletin (5,6,7,8,3',4'-hexamethoxyflavone).

4. MAPK family

The mitogen-activated protein kinase (MAPK) family, which includes extracellular regulated kinases 1/2 (ERK1/2), p38 mitogen-activated protein kinase (p38MAPK), Jun amino terminal kinase (JNK), is involved in the regulation of various cellular responses, such as cell proliferation, survival, apoptosis, and inflammation [2, 30]. Particularly, in keratinocytes, p38MAPK activation

promotes UVB-induced apoptosis [2]. Furthermore, keratinocyte proliferation and differentiation are well controlled by ERK1/2 and p38MAPK. The ERK pathway promotes cell proliferation and regulates cell survival, while the p38MAPK pathway induces apoptosis and differentiation [31]. ERK signaling is involved in a wide variety of cellular responses, including not only cell proliferation and survival (anti-apoptotic activity) but also differentiation and migration [32, 33]. A previous study showed that ETS domain-containing protein (Elk-1), the transcription factor, activated by ERK1/2 induces expression of Egr-1 which promotes cell proliferation and suppresses apoptosis in keratinocytes [34]. Moreover, it has been reported that the expression of involucrin, a keratinocyte differentiation marker, in response to calcium is sensitive to inhibition of the ERK pathway [35], and that ERK1/2 regulates cell migration of keratinocytes through the activation of focal adhesion kinase [36]. Additionally, oncogenic Ras has been shown to be involved in the growth and development of human cutaneous squamous cell carcinoma (cSCC) through the activation of the ERK pathway [37]. Therefore, the identification and characterization of compounds that can modulate MAPK signaling in keratinocytes may help in developing novel drugs for treating skin diseases.

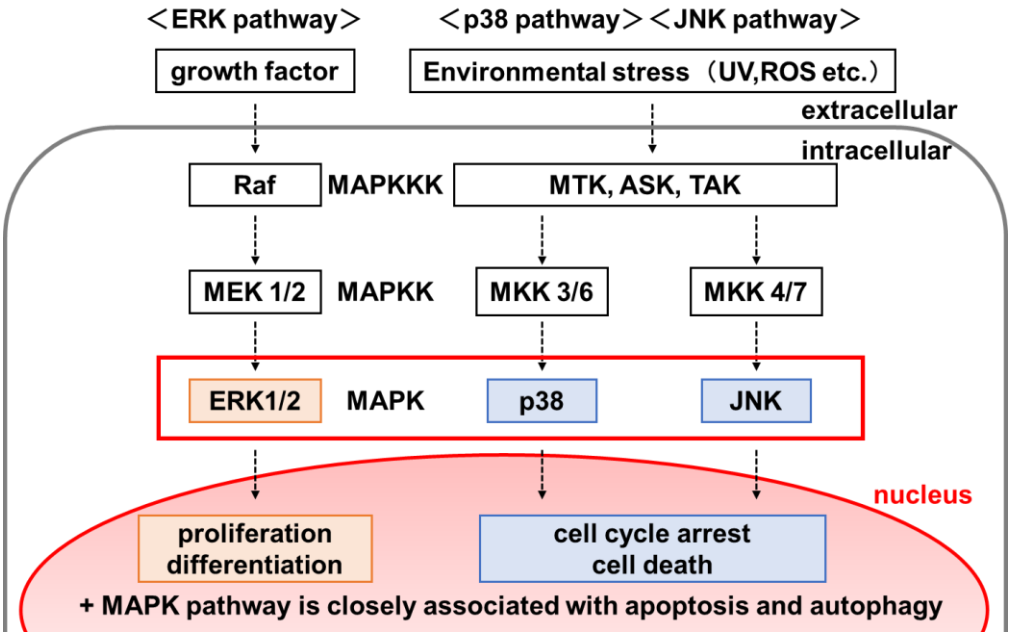

Figure 5. MAPK pathway.

Chapter 2　Sudachitin and nobiletin induce distinct cellular responses

1.　Introduction

In multicellular organisms, cell death is an important process that maintains tissue homeostasis and eliminates potentially harmful cells [6]. There are various modalities of cell death, including apoptosis (type I), autophagic cell death (type II), and necrosis (type III) [7]. Apoptosis also plays a pivotal role in eliminating genetically damaged cells that might progress to cancer. On the other hand, autophagy constitutively occurs at low levels to degrade cytoplasmic components to maintain homeostasis. However, overactivation of autophagy may result in autophagic cell death, autophagy dysfunction is associated with a number of diseases, including infection, cancer, and neurodegeneration. Therefore, there have been conducted many trials to develop new compounds that induce either apoptosis or autophagy.

A wide variety of polyphenols have been identified in many plants, including citrus fruits, cocoa, and tea [38, 39]. Several studies have shown that most of them exhibit biological activities, including antioxidant and anticancer effects. Some natural polyphenolic compounds, such as genistein and curcumin, induce apoptosis and autophagy [40]. PMF, a class of flavonoid compounds that are almost exclusively found in the peel of citrus fruits, also possess various biological activities [19, 20]. For example, nobiletin (Figure 4, right), which is a typical PMF from the peel of *C. depressa* and has been reported to induce apoptosis and autophagy in human gastric cancer cells [41]. Other PMFs, sudachitin (Figure 4, left) and 3’-demethoxysudachitin (Figure 4, middle), have been isolated from the peel of *C. sudachi* [25]. Although previous report showed that sudachitin possesses an anti-inflammatory activity, their other biological activities are not yet fully understood [26]. In chapter 2, I attempted to elucidate novel biological activities of sudachitin and 3’-demethoxysudachitin.

2. Materials and methods

2.1. Materials

Sudachitin, nobiletin (Wako Pure Chemical Industries), and 3'-demethoxysudachitin [42] were dissolved in 100% dimethyl sulfoxide (DMSO) at a concentration of 100 mM, and the final concentration of DMSO in the culture medium was 0.1%.

2.2. Cell culture

Human adult low-calcium high-temperature (HaCaT) cells, from an immortalized human keratinocyte cell line developed by the German Cancer Research Center (Deutsches Krebsforschungszentrum, DKFZ) [43] and murine B16 melanoma cells (B16 cells) were cultured in Dulbecco's Modified Eagle's Medium (DMEM) (FUJIFILM Wako Pure Chemical Corporation) supplemented with 10% fetal bovine serum (FBS) (MP Biomedicals), 100 units/mL penicillin, and 100 µg/mL streptomycin at 37 °C in a humidified incubator with 5% CO_2.

2.3. MTT assay

HaCaT cells and B16 cells were seeded in 96-well culture plates. After 24 hours, the cells were treated with 30 or 100 µM sudachitin, 3'-demethoxysudachitin, nobiletin, or DMSO for 24 and 48 hours. After 1-hour incubation with 3-(4,5-dimethyl-2-thiazolyl)-2,5-diphenylte-trazolium bromide (MTT), the resulting formazan crystals were dissolved in DMSO. The absorbance at 570 nm (650 nm as a reference) was determined using the Infinite M200 plate reader (TECAN Japan).

2.4. Immunoblot analysis

Cells were treated with sudachitin (30, 100 µM), 3'-demethoxysudachitin (30, 100 µM), nobiletin (30, 100 µM), or DMSO for 24 and 48 hours. Then the cells were lysed in an ice-

cold TNE buffer consisting of 20 mM Tris-HCl (pH 7.5), 150 mM NaCl, 0.5% Nonidet P-40, 1 mM ethylenediaminetetraacetic acid (EDTA), and protease inhibitors (10 μg/mL leupeptin and 10 μg/mL aprotinin). The protein extracts were clarified by centrifugation at 10,000 × g for 10 min. Protein amounts were quantitated by BCA protein assay (Thermo Fisher Scientific). The absorbance of sample after reaction at 562 nm was determined using the Infinite M200 plate reader (TECAN Japan). The amount of protein was calculated by a calibration curve which prepared using 2 mg / ml BSA as a standard. The equal amount of protein was mixed with a 6 x SDS-loading buffer and heat-treated at 95 °C for 5 minutes. The heat-treated protein was subjected to SDS-PAGE and immunoblotting with antibodies against microtubule-associated protein light chain 3 (LC3), glyceraldehyde-3-phosphate dehydrogenase (GAPDH) (Wako Pure Chemical Industries), or poly (ADP-ribose) polymerase (PARP) (Cell Signaling Technology). The luminescent signals were analyzed using LAS-4000 image analyzer (Fuji Film).

2.5. Apoptosis assay by annexin V/propidium iodide (PI) staining

HaCaT cells were treated with sudachitin (30, 100 μM), 3'-demethoxysudachitin (30, 100 μM), nobiletin (30, 100 μM), or DMSO for 24 and 48 hours. Cells were detached from the culture dish by trypsin/EDTA treatment and washed with culture medium and phosphate buffered saline (PBS). Annexin V-FITC and PI stating was performed using a MEBCYTO Apoptosis Kit (Medical & Biological Laboratories) according to the manufacturer's instructions. The samples were analyzed by flow cytometry (BD FACSVerse system, BD Biosciences).

2.6. Immunofluorescence analysis

HaCaT cells and B16 cells were treated with 100 μM nobiletin, sudachitin, or DMSO. After 24 or 48 hours, cells were fixed using 3.7% formaldehyde for 20 minutes, permeabilized with 0.1% Triton X-100 for 5 minutes, and then blocked in 5% BSA overnight. Cells were subsequently

incubated with mouse anti-LC3 antibody (Wako Pure Chemical Industries) overnight at 4 °C. After washing with PBS, cells were incubated for 1 hour with Alexa Fluor 488-conjugated goat anti-rabbit IgG antibody (Thermo Fisher Scientific). Fluorescent images were obtained using an IN Cell Analyzer 6000 system (GE Healthcare).

2.7. Autolysosome detection

HaCaT cells and B16 cells were treated with 1 μM DALGreen (Dojindo Laboratories) at 37 °C for 30 min. Then the culture medium was removed, and cells were incubated in culture medium containing 100 μM nobiletin at 37 °C for 24 or 48 hours. Cells were observed by IN Cell Analyzer 6000 to obtain fluorescence images.

2.8. Statistical analysis

All experiments were performed multiple times to confirm their reproducibility. One representative set of data was shown in the figures. Immunoblot band intensities were quantified using Image J software (NIH). Data were expressed as the mean ± standard error (SE), and statistical analysis was performed by Student's t-test or one-way analysis of variance (ANOVA) with Tukey's multiple comparison tests using GraphPad Prism (GraphPad Software).

3. Results

3.1. Effect of sudachitin and nobiletin on the proliferation of keratinocytes

In order to assess the effects of sudachitin (5,7,4’-trihydroxy-6,8,3’-trimethoxyflavone) (Figure 4, left) and 3’-demethoxy-sudachitin (5,7,4’-trihydroxy-6,8-dimethoxyflavone) (Figure 4, middle) on cell proliferation in keratinocytes, immortalized human keratinocyte HaCaT cells were treated with 30 or 100 μM sudachitin or 3’-demethoxysudachitin for 24 and 48 hours and then subjected to an MTT assay. As shown in Figure 6, sudachitin significantly suppressed the proliferation of HaCaT cells in a dose-dependent manner. Although 3’-demethoxysudachitin exhibited an antiproliferative activity at a concentration of 100 μM, little effect was observed at 30 μM. Additionally, their analogous compound, nobiletin (5,6,7,8,3’,4’-hexamethoxyflavone) (Figure 4, right), was also tested, resulting in significant growth suppression at 30 and 100 μM. The results showed that three PMFs suppressed the proliferation of HaCaT cells at a high concentration (100 μM).

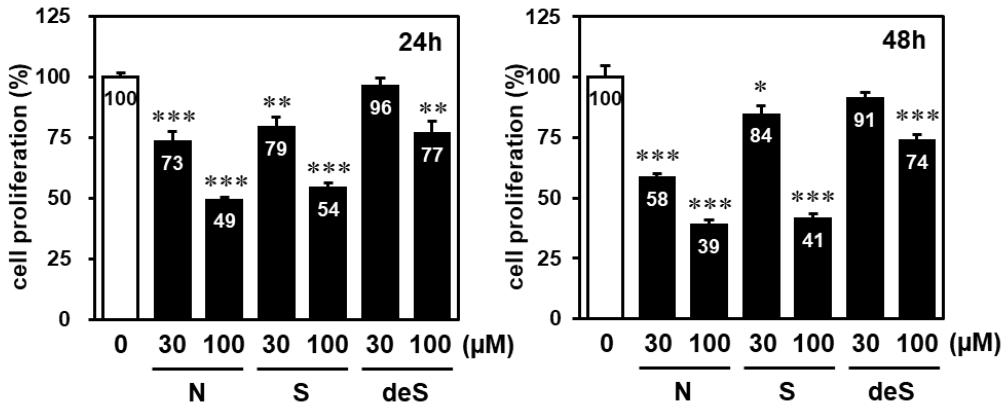

Figure 6. Effect of sudachitin, 3’-demethoxysudachitin, and nobiletin on cell proliferation of HaCaT cells.

HaCaT cells were treated with sudachitin (*S*) (30, 100 μM), 3’-demethoxysudachitin (*deS*) (30, 100 μM), nobiletin (*N*) (30, 100 μM) or DMSO (*C*). After 24 hours (left panel) and 48 hours (right panel), cell proliferation was measured by MTT assay. Results are expressed relative to cells treated with DMSO (= 100%). The data are expressed as the mean ± SE for at least four cultures, and statistical analysis was performed by Student’s t-test. *** $p < 0.001$, ** $p < 0.01$, and * $p < 0.05$ compared with cells treated with DMSO.

3.2. Sudachitin specifically induces apoptosis in a concentration- and time-dependent manner in keratinocytes

Next, I examined whether these PMFs induce apoptosis. Due to the fact that PARP (116 kDa) is cleaved to fragments of molecular sizes of 85 and 27 kDa by activated caspase-3 in response to apoptotic signals, the cleavage of PARP is widely used as an apoptotic marker [44]. Immunoblotting analysis with an anti-PARP antibody revealed that the amount of cleaved PARP significantly increased in HaCaT cells treated with 100 μM sudachitin, but not in those treated with 3'-demethoxysudachitin and nobiletin at an equivalent concentration (Figure 7(A)). As shown in Figure 7(B, C), sudachitin induced PARP cleavage in a concentration- and time-dependent manner. In order to obtain further evidence that sudachitin induces the apoptosis of HaCaT cells, sudachitin-treated cells were subjected to annexin V-FITC/PI staining and analyzed by flow cytometry. As shown in Figure 7(D, E), the percentages of annexin V-positive/PI-negative cells, indicative of early apoptosis, were significantly increased to 26% and 41%, respectively, when cells were treated with 100 μM sudachitin for 24 and 48 hours, compared with DMSO treatment (5.9% and 6.5%). In contrast, nobiletin and 3'-demethoxysudachitin hardly affected. I also examined the dose dependence of the effect of sudachitin on induction of early apoptosis. As shown in Figure 7(D, F), sudachitin promoted early apoptosis in a concentration-dependent manner. Additionally, the percentage of the sum of early apoptotic (annexin V-positive/PI-negative) and late apoptotic/necrotic (annexin V-positive/PI-positive) cells was also calculated. As shown in Figure 7(G), the percentage significantly increased to approximately 80% in the cells treated with 100 μM sudachitin for 48 hours, which almost correlated with the percentage of cleaved PARP (84-94%) in Figure 7(A-C). These results show that sudachitin but not 3'-demethoxysudachitin and nobiletin specifically induces apoptosis.

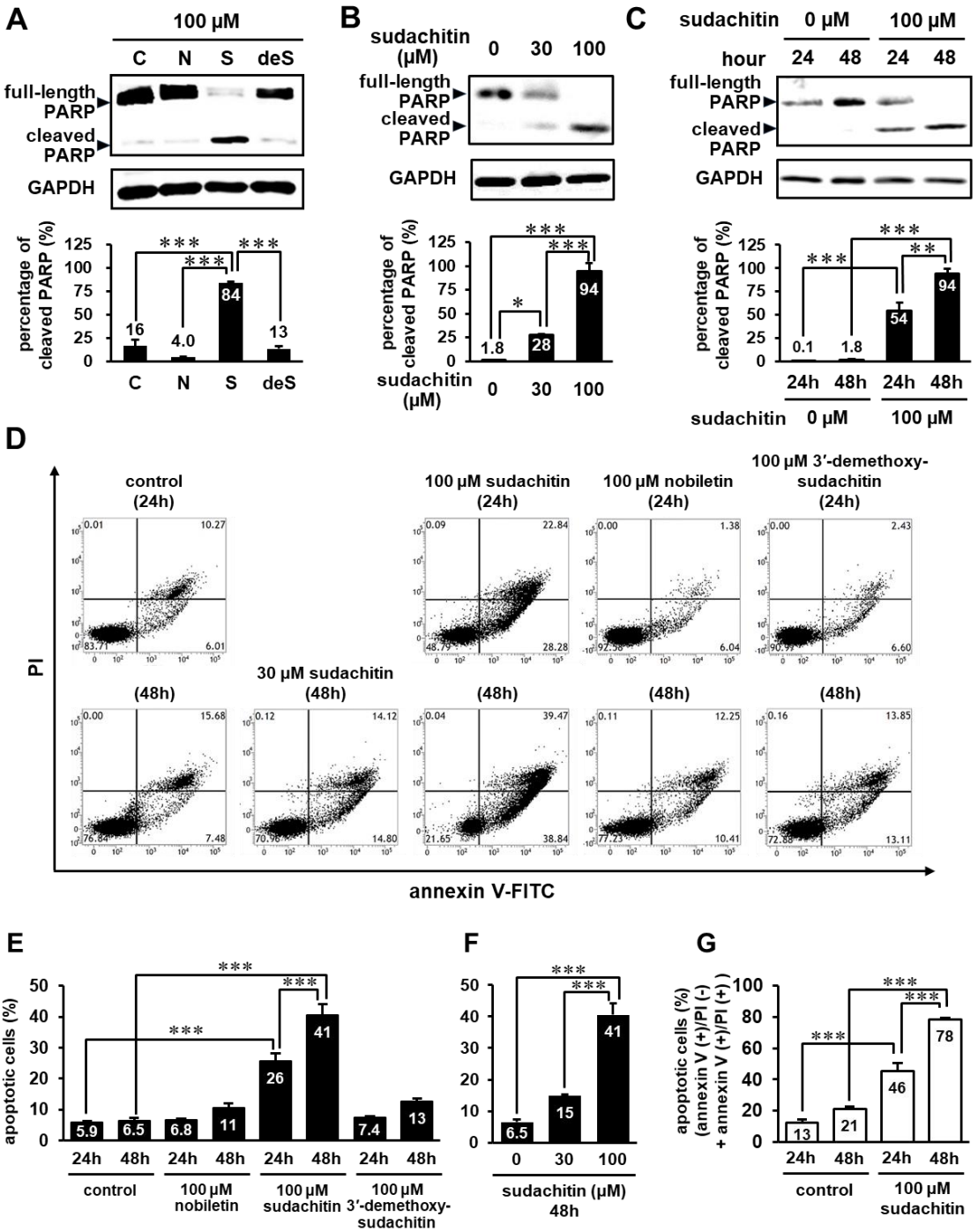
A
100 μM
C N S deS
full-length PARP
cleaved PARP
GAPDH
percentage of cleaved PARP (%)
16 4.0 84 13
C N S deS
B
sudachitin (μM) 0 30 100
full-length PARP
cleaved PARP
GAPDH
percentage of cleaved PARP (%)
1.8 28 94
sudachitin (μM) 0 30 100
C
sudachitin 0 μM 100 μM
hour 24 48 24 48
full-length PARP
cleaved PARP
GAPDH
percentage of cleaved PARP (%)
0.1 1.8 54 94
24h 48h 24h 48h
sudachitin 0 μM 100 μM
D
control (24h)
100 μM sudachitin (24h)
100 μM nobiletin (24h)
100 μM 3′-demethoxy-sudachitin (24h)
30 μM sudachitin (48h)
(48h)
PI
annexin V-FITC
E
annexin V (+)/PI (-) apoptotic cells (%)
5.9 6.5 6.8 11 26 41 7.4 13
24h 48h 24h 48h 24h 48h 24h 48h
control
100 μM nobiletin
100 μM sudachitin
100 μM 3′-demethoxy-sudachitin
F
6.5 15 41
0 30 100
sudachitin (μM) 48h
G
apoptotic cells (%) (annexin V (+)/PI (-) + annexin V (+)/PI (+))
13 21 46 78
24h 48h 24h 48h
control
100 μM sudachitin

Figure 7. Sudachitin specifically induces apoptosis in a concentration- and time-dependent manner.

(A) HaCaT cells were stimulated with 100 μM nobiletin (*N*), 100 μM sudachitin (*S*), 100 μM 3'-demethoxysudachitin (*deS*), or DMSO (*C*) for 48 hours. (B and C) HaCaT cells were treated with 30 and 100 μM sudachitin for 24 and 48 hours. The cell lysates were analyzed by immunoblotting using anti-PARP and anti-GAPDH antibodies. The detected bands were quantitated by ImageJ software, and the percentage of cleaved PARP (associated to apoptosis) relative to the total amount of PARP (full-length plus cleaved PARP) was quantified. (D) HaCaT cells were treated with sudachitin (30, 100 μM), nobiletin (100 μM), 3'-demethoxysudachitin (100 μM), or DMSO (control) for 24 or 48 hours. The cells were stained by annexin V-FITC and PI, and were analyzed using flow cytometry. (E and F) The amount of early apoptosis were determined as the percentage of annexin V (+)/PI (-) (the lower right quadrants of flow cytometric assay). (G) The percentage of both annexin V (+)/PI (-) (early apoptosis) and annexin V (+)/PI (+) (late apoptosis/necrosis) cells were shown. The data were expressed as the mean ± SE, and statistical analysis was performed by one-way ANOVA with Tukey's multiple comparison tests. *** $p < 0.001$, ** $p < 0.01$, * $p < 0.05$.

3.3. Nobiletin specifically triggers autophagy in keratinocytes

Some natural polyphenolic compounds, such as genistein, quercetin, curcumin, and resveratrol, are known to induce not only apoptosis but also autophagy [40]. Furthermore, it was reported that nobiletin induces apoptosis-mediated protective autophagy in human gastric cancer SNU-16 cells [41]. Therefore, I examined whether nobiletin, sudachitin, and 3'-demethoxysudachitin induce autophagy in HaCaT cells. During the formation of autophagosomes, LC3-I is converted into LC3-II conjugated to phosphatidylethanolamine and recruited to the autophagosome membrane, although LC3-I is diffusely distributed in the cytoplasm under normal conditions [10, 45]. The conversion of LC3-I into LC3-II through proteolytic cleavage and lipidation is a hallmark of autophagy, which can be quantified by immunoblotting analysis with an anti-LC3 antibody. As shown in Figure 8(A, B), the level of LC3-II was significantly increased by treatment with nobiletin (30 and 100 μM) in HaCaT cells. On the other hand, 3'-demethoxysudachitin and sudachitin failed to induce autophagy. I subsequently confirmed that nobiletin induces autophagy by immunofluorescence analysis with an anti-LC3 antibody and cell staining with DALGreen, which is a fluorescent probe for monitoring the formation of autolysosomes [46]. Immunofluorescence analysis showed that LC3 puncta, which represent autophagosome formation, were observed in

HaCaT cells treated with 100 μM nobiletin (Figure 8(C)). Furthermore, an increase in DALGreen fluorescence was observed in cells treated with nobiletin (Figure 8(D)). These results show that three PMFs have different effects on apoptosis and autophagy.

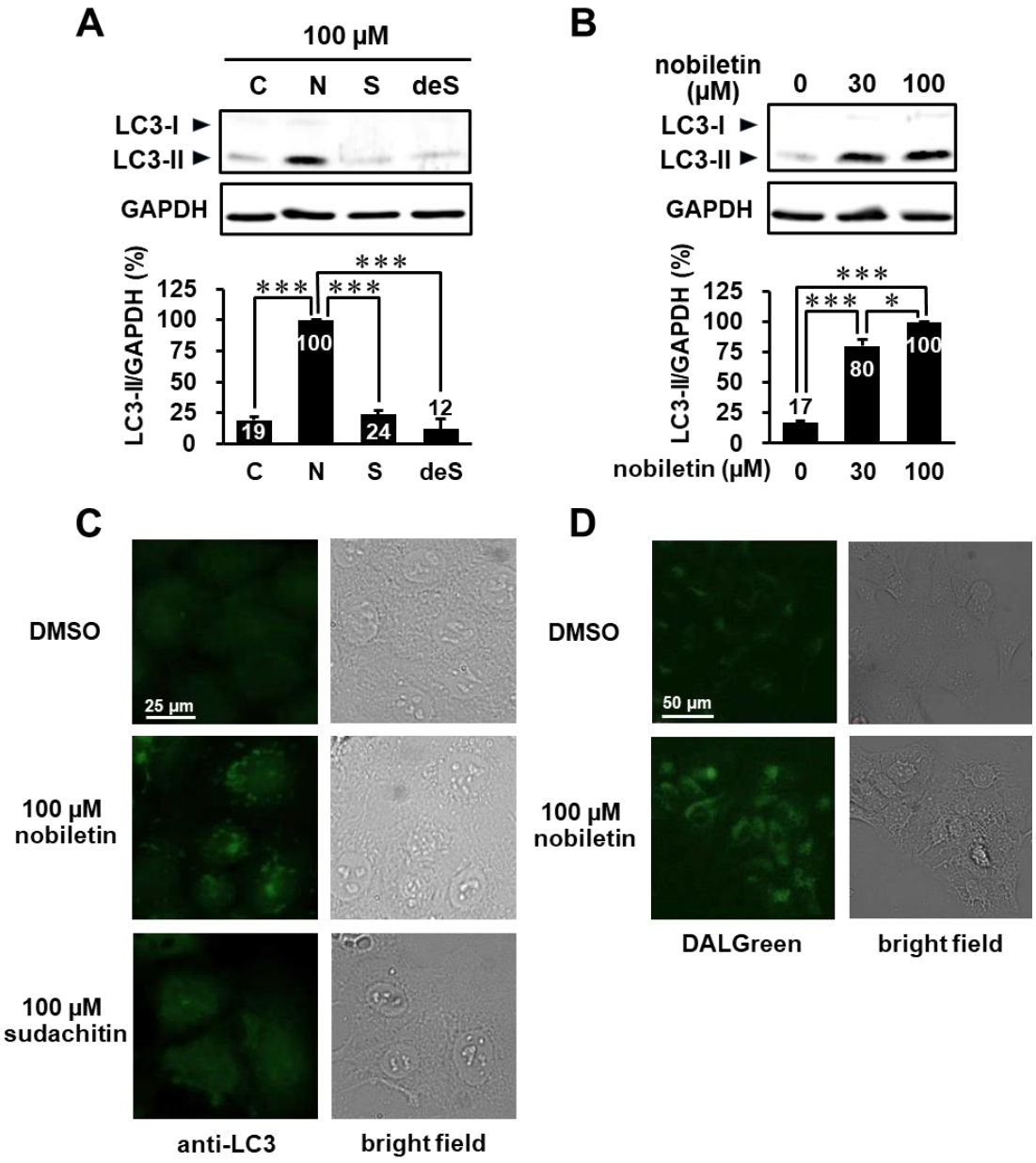

Figure 8. Nobiletin specifically triggers autophagy in HaCaT cells.

(A) HaCaT cells were treated with 100 μM nobiletin (*N*), 100 μM sudachitin (*S*), 100 μM 3'-demethoxysudachitin (*deS*), or DMSO (*C*) for 48 hours. (B) HaCaT cells were stimulated with nobiletin (30, 100 μM) or DMSO for 48 hours. The cell lysates were analyzed by immunoblotting using anti-LC3 and anti-GAPDH antibodies. The detected bands were quantitated by ImageJ software, and quantification of results is presented as the amount of LC3-II normalized against GAPDH. The data are expressed as means ± SE of three separate experiments, and statistical analysis was performed by one-way ANOVA with Tukey's multiple comparison tests. *** $p < 0.001$, * $p < 0.05$. (C and D) HaCaT cells were stimulated with 100 μM nobiletin, 100 μM sudachitin, or DMSO for 24 hours, and were subjected to immunofluorescence with an anti-LC3 antibody (C) and DALGreen staining (D). All experiments were performed multiple times with similar results.

3.4. Effect of PMFs on B16 melanoma cells

Next, I assessed potential antiproliferative activities of sudachitin and nobiletin on melanoma cells, mouse B16 melanoma cells. B16 cells were treated with 30 or 100 μM sudachitin for 48 hours and then used in MTT assay. As shown in Figure 9(A), B16 cells treated with both sudachitin and nobiletin were significantly suppressed cell proliferation in a dose-dependent manner. This result showed that both sudachitin and nobiletin suppressed cell proliferation in B16 cells in a concentration of 100 μM. Moreover, I examined whether sudachitin and nobiletin be able to induce apoptosis and autophagy in B16 cells. Interestingly, unlike the results in HaCaT cells, no cleaved PARP was detected, and the level of LC3-II was significantly increased by treatment with both sudachitin (100 μM) and nobiletin (100 μM) in B16 cells (Figure 9(B, C)). These results indicated that B16 cells are resistant to sudachitin-induced apoptosis, on the other hands, not are resistant to autophagy induced by three PMFs. Furthermore, I confirmed that sudachitin induces autophagy in B16 cells by immunofluorescence analysis with anti-LC3 antibody and cell staining with DALGreen. Immunofluorescence analysis showed that LC3 puncta were observed in cells treated with 100 μM sudachitin (Figure 9(D)). Additionally, an increase of DALGreen fluorescence was observed in B16 cells treated with sudachitin (Figure 9(E)). These results suggested that sudachitin promotes cell-type specific autophagy, while nobiletin may induce autophagy in a wide range of cells.

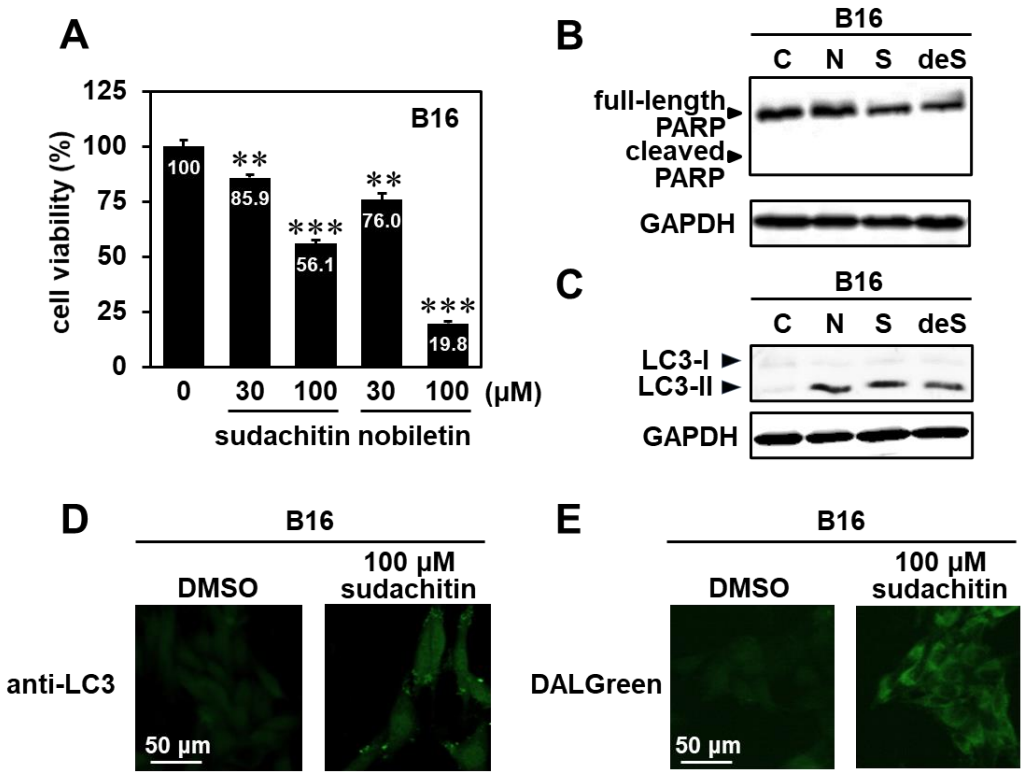

Figure 9. Three PMFs induce autophagy in B16 cells.

(A) B16 cells were treated with sudachitin (*S*) (30, 100 μM) and nobiletin (*N*) (30, 100 μM) or DMSO (*C*). After 48 hours, cell proliferation was measured by MTT assay. Results are expressed relative to cells treated with DMSO (= 100%). The data are expressed as the mean ± SE for at least four cultures, and statistical analysis was performed by Student's t-test. *** $p < 0.001$, ** $p < 0.01$, and * $p < 0.05$ compared with cells treated with DMSO. (B and C) B16 cells were stimulated with 100 μM nobiletin (*N*), 100 μM sudachitin (*S*), 100 μM 3'-demethoxysudachitin (*deS*), or DMSO (*C*) for 48 hours. The cell lysates were analyzed by immunoblotting using anti-PARP, anti-GAPDH, and anti-LC3 antibodies. (D and E) B16 cells were stimulated with 100 μM sudachitin, or DMSO for 24 hours, and were subjected to immunofluorescence with an anti-LC3 antibody (C) and DALGreen staining (D). All experiments were performed multiple times with similar results.

4. Discussion

A wide range of compounds that regulate apoptosis and/or autophagy have been identified and are expected to act as anticancer agents [47]. Natural polyphenolic compounds isolated from plants could also affect apoptosis and autophagy [40, 19, 23, 41]. Due to the fact that the avoidance of cell death is closely related to the promotion and progression of cancer, it is important to identify and characterize compounds that can regulate cell death processes. In this study, I demonstrated that sudachitin (5,7,4’-trihydroxy-6,8,3’-trimethoxyflavone), a PMF isolated from the peel of *C. sudachi*, could induce apoptosis in human keratinocyte HaCaT cells. On the other hand, nobiletin (5,6,7,8,3’,4’-hexamethoxyflavone) could induce autophagy, whereas it failed to promote apoptosis. Additionally, 3’-demethoxysudachitin (5,7,4’-trihydroxy-6,8-dimethoxy-flavone) did not induce apoptosis or autophagy.

Citrus PMFs are flavones that bear two or more methoxy groups on their basic benzo-γ-pyrone skeleton with a carbonyl group at the C-4 position [48]. Maximum number of the methoxy groups can be up to seven (3,5,6,7,8,3’,4’-heptamethoxyflavone and 5,6,7,8,3’,4’,5’-heptamethoxy-flavone), and one or more methoxy group(s) is (are) replaced by hydroxyl group(s) (hydroxylated PMF or demethyl PMF). The number and positions of methoxy group greatly influence the biological functions of PMFs. For example, although nobiletin has an anti-apoptotic effect in human neuroblastoma SH-SY5Y cells, 5-demethylnobiletin (5-hydroxy-6,7,8,3’,4’-pentamethoxyflavone), which is demethylated at the 5-methoxy group in nobiletin, exhibits a growth inhibitory effect [49]. These data suggest that the methoxy group at the C-5 position of nobiletin may contribute to the anti-apoptotic effect, and that hydroxylated PMFs may effectively induce cell death. Sudachitin is also a hydroxylated PMF, which the methoxy groups at the C-5, C-7, and C-4’ positions in nobiletin are replaced by the hydroxyl groups, and therefore, sudachitin but not nobiletin may exhibit pro-apoptotic activity. On the other hand, 3’-demethoxysudachitin only slightly suppressed cell proliferation in HaCaT cells. Although 5-demethylnobiletin can

strongly induce apoptosis in HL-60 leukemia cells, neither tangeretin (5,6,7,8,4'-pentamethoxyflavone) nor 5-demethyltangeretin (5-hydroxy-6,7,8,4'-tetramethoxy-flavone) affects cell proliferation [50]. Taken together, the methoxy group at the C-3' position may exhibit a growth inhibitory effect. Further study will be required to elucidate the related structure-activity relationship of other PMFs.

Although I demonstrated that nobiletin did not induce apoptosis in HaCaT cells, it has been reported that nobiletin promotes apoptosis by suppressing MAPKs in human breast cancer cell lines [51]. Previous studies showed that some compounds induced cell-type-specific apoptosis and autophagy [52, 53]. For example, honokiol, a natural biphenolic compound derived from the bark of magnolia trees, induces apoptosis and autophagy via the reactive oxygen species (ROS) signaling pathway in human osteosarcoma, whereas it does not induce cell death in normal human primary skin fibroblasts [52]. Furthermore, a green tea polyphenol analog, JP8, preferentially induces cell death in cancer cells, such as murine B16 melanoma cells [53]. JP8 can apparently induce selective ROS accumulation in cancer cells but not in normal cells, resulting in autophagic cell death. Interestingly, I found that, in B16 melanoma cells, sudachitin fails to induce apoptosis and triggers autophagy. A more recent study showed that sudachitin decreases the activation of MAPKs and the ROS production evoked by the receptor activator of nuclear factor-kappa B (NF-κB) ligand in osteoclasts [27], suggesting that sudachitin may also induce apoptosis and autophagy through a pathway such as ROS production.

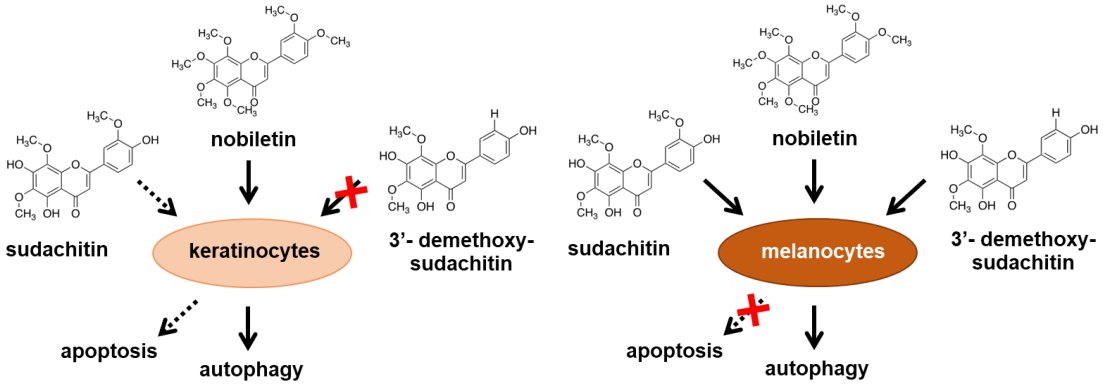

Figure 10. Three PMFs have different effects on apoptosis and autophagy in skin cells.

Chapter 3 Sudachitin induces apoptosis via the regulation of MAPK pathways

1. Introduction

A previous study demonstrated that sudachitin could exert its biological activity via the regulation of the MAPK pathways [27]. Sudachitin suppresses inflammatory bone destruction by inhibiting receptor activator of NF-κB ligand (RANKL)-induced ERK1/2 and JNK activations. However, a study reported contradictory results that sudachitin did not affect tumor necrosis factor (TNF)-α-induced activation of MAPK family members [28]. Thus, the effect of sudachitin on MAPK signaling pathways remains controversial and unclear. In chapter 2, I reported that in human keratinocyte HaCaT cells, sudachitin and nobiletin can induce apoptosis and autophagy, respectively, indicating that the two PMFs induce distinct cellular responses despite small structural differences. Other studies suggested that hydroxylated PMFs, in which some of the methoxy groups are replaced by a hydroxyl group, show a higher ability to induce apoptosis than non-hydroxylated PMFs [54, 55]. These PMFs include 3,5-dihydroxy-6,7,3’4’-tetramethoxy-flavone and 5-demethyltangeretin (5-hydroxy-6,7,8,4’-tetramethoxy-flavone). Although the methoxy groups at the C-3’ and C-8 positions may be involved in the induction of apoptosis (chapter 2 Discussion), the structure-activity relationship and molecular mechanism underlying PMF-induced apoptosis are not yet fully elucidated. Understanding the mechanisms of distinct cellular responses caused by small structural differences in PMFs may lead to the discovery of more effective apoptotic inducers and identify different biological activities of PMFs. In chapter 3, I investigated the mechanism underlying sudachitin-induced apoptosis via the MAPK pathways.

2. Materials and methods

2.1. Materials

Sudachitin and nobiletin (Wako Pure Chemical Industries) were dissolved in 100% DMSO, and cells were exposed to a final concentration of 0.1% DMSO. epidermal growth factor (EGF) (Peptide Institute) and mitomycin C were dissolved in sterile water, while N-benzyloxycarbonyl-Val-Ala-Asp(O-Me) fluoromethyl ketone (z-VAD-FMK) (Peptide Institute) and SB203580 (Calbiochem) were dissolved with DMSO.

2.2. Cell culture

HaCaT cells, from an immortalized human keratinocyte cell line developed by the German Cancer Research Center (Deutsches Krebsfors-chungszentrum, DKFZ) [43], were cultured in DMEM (FUJIFILM Wako Pure Chemical Corporation) supplemented with 10% FBS (MP Biomedicals), 100 units/mL penicillin, and 100 μg/mL streptomycin at 37 °C in a humidified incubator with 5% CO_2.

2.3. Immunoblot analysis

Immunoblot analysis was performed as described in chapter 2. Cells were treated with sudachitin (30, 100 μM), nobiletin (100 μM), or DMSO for different time periods. Total cell lysates were prepared and subjected to immunoblot analysis using antibodies against BH3-interacting-domain death agonist (Bid), cleaved caspase-3, PARP, total/phospho-ERK1/2, total/phospho-p38MAPK, total/phospho-JNK, total/phospho- MAP kinase 3/6 (MKK3/6), phospho-HSP27, phospho-Raf-1 (Ser-338) (Cell Signaling Technology), Raf-1 (BD Transduction Laboratories), or GAPDH (Wako Pure Chemical Industries). Immunoblot band intensities were quantified using the ImageJ software (NIH).

2.4. Luciferase reporter assay

HaCaT cells were plated in a 24-well plate, and were transfected with pFR-Luc, pFA2-Elk1, and pCMV-β-gal using FuGENE HD (Roche) according to the manufacturer's instructions. After serum-starvation for 2 h and subsequent treatment with 30 μM sudachitin for 1 h, cells were stimulated with 1 nM EGF for an additional 6 h. After harvest, luciferase and *β*-galactosidase activities were measured using the Promega's luciferase system and *o*-nitrophenyl-*β*-*D*-galactopyranoside, respectively. Luciferase activity was normalized to β-galactosidase activity.

2.5. *In vitro* wound healing assay

HaCaT cells were seeded on a 24-well plate. After cells were grown to confluence, the culture medium was replaced with serum-free medium for 2 h. Then, cells were pretreated with DMSO or 30 μM sudachitin in the presence of 10 μg/ml mitomycin C. After 1 h, the confluent monolayers were scratched with a yellow pipette tip. The detached cells were removed by washing with PBS three times. Subsequently, cells were treated with DMSO or 30 μM sudachitin in the presence or absence of 1 nM EGF for 24 h. Images were captured in the same position at 0 and 24 h after the scratch using an IN Cell Analyzer 6000 system (GE Healthcare), and the wound areas were quantified using ImageJ software. The migration area was calculated as the difference between the initial and final wound area.

2.6. BrdU proliferation assay

Cell proliferation was measured by 5-bromo-2'-deoxyuridine (BrdU) incorporation assay using a CycLex Cellular BrdU ELISA Kit Ver.2 (Medical & Biological Laboratories) according to the manufacturer's instructions. Briefly, HaCaT cells were plated on 96-well plates and were serum-starved for 24 h. After pretreatment with 10 μM sudachitin for 1 h, cells were treated with 1 nM EGF. After 24 h, the cells were incubated with BrdU for 2 h. Following treatment with anti-BrdU

antibody and substrate, the absorbance at 450 nm with 540 nm as reference was measured using the Infinite M200 plate reader (TECAN Japan).

2.7. Statistical analysis

All experiments were performed multiple times to confirm their reproducibility. One representative set of data was shown in the figures, and data were expressed as the mean ± SE. Statistical analysis was performed by one-way ANOVA followed by Tukey's or Bonferroni's multiple comparison tests using GraphPad Prism (GraphPad Software).

3. Results

3.1. Sudachitin induces caspase-dependent apoptosis in HaCaT cells

I reported that sudachitin and nobiletin induce apoptosis and autophagy in HaCaT cells, respectively, in chapter 2. However, the mechanisms underlying apoptosis are not yet fully understood. In chapter 3, I aimed to characterize the molecular pathways underlying sudachitin-induced apoptosis. To confirm the apoptotic effect of sudachitin, I measured caspase activation in HaCaT cells using immunoblot analysis. Consistent with results of chapter 2, sudachitin induced PARP cleavage, which is dependent on caspase-3 activation and is an apoptotic hallmark, in a concentration-dependent manner (Figure 11(A)). Sudachitin also caused a dose-dependent proteolytic cleavage and the activation of caspase-3. Bid is a pro-apoptotic Bcl-2 family protein activated by caspase-8. Sudachitin significantly decreased the level of full-length Bid, accompanied by an increased amount of its cleaved product, truncated Bid (tBid). Furthermore, HaCaT cells were pretreated with the pan-caspase inhibitor z-VAD-FMK prior to being exposed to sudachitin. As shown in Figure 11(B), z-VAD-FMK significantly reduced the sudachitin-induced cleavage of PARP, further reinforcing that sudachitin induces apoptosis via the caspase pathway. These results indicated that sudachitin induces apoptosis via the caspase pathway

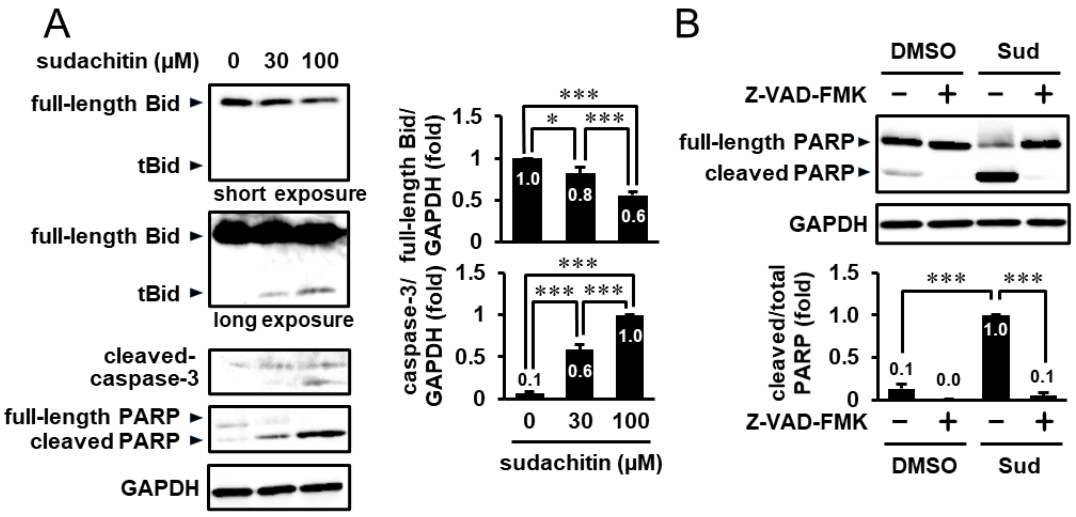

Figure 11. Sudachitin induces caspase-mediated apoptosis.

(A) HaCaT cells were stimulated with sudachitin (30 and 100 μM) or DMSO for 24 h. (B) After pretreatment with 50 μM z-VAD-FMK for 1 h, HaCaT cells were treated with 30 μM sudachitin (Sud) for 24 h. The cell lysates were subjected to immunoblot analysis with antibodies specific for the indicated proteins, and the detected bands were quantitated by ImageJ software. The levels of full-length Bid and cleaved caspase-3 were normalized to those of GAPDH. The levels of cleaved PARP were normalized to that of full-length PARP. The data were expressed as the mean ± SE derived from at least three independent experiments, and statistical analysis was performed by one-way ANOVA with either Tukey's (A) or Bonferroni's (B) multiple comparison. ***$p < 0.001$, *$p < 0.05$.

3.2. Sudachitin regulates MAPK pathways in HaCaT cells

Previous studies have demonstrated that some polyphenolic compounds induce apoptosis by modulating the MAPK pathways (e.g., ERK1/2, p38MAPK, and JNK) [56, 57]. Therefore, I assessed whether sudachitin-induced apoptosis is also associated with the ERK1/2, p38MAPK, and JNK pathways. Sudachitin increased p38MAPK and JNK phosphorylation, but significantly decreased ERK1/2 phosphorylation (Figure 12). In contrast, nobiletin significantly increased ERK1/2 phosphorylation. These results suggest that sudachitin induces apoptosis through different signaling pathways from nobiletin.

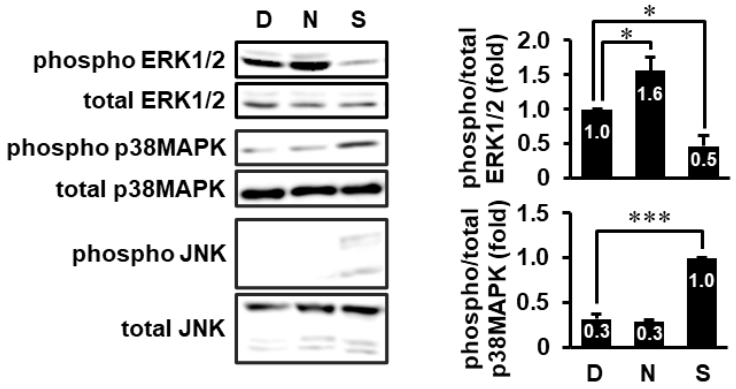

Figure 12. sudachitin regulates MAPK pathways.

HaCaT cells were stimulated with 100 μM nobiletin (N), 100 μM sudachitin (S), or DMSO (D) for 4 h. The cell lysates were subjected to immunoblot analysis with antibodies specific for the indicated proteins, and the detected bands were quantitated by ImageJ software. The levels of phosphorylated MAPKs were normalized to that of total MAPKs, respectively. The data were expressed as the mean ± SE derived from at least three independent experiments, and statistical analysis was performed by one-way ANOVA with Bonferroni's multiple comparison. ***$p < 0.001$, *$p < 0.05$.

3.3. Sudachitin induces apoptosis via the activation of the p38MAPK pathway

A previous study has revealed that p38MAPK plays an important role in chemotherapeutic agent-induced apoptosis [58]. As sudachitin, not nobiletin, induced p38MAPK phosphorylation and activation, I next examined the dose-dependence of the effect of sudachitin on p38MAPK phosphorylation. Sudachitin promoted p38MAPK phosphorylation in a concentration-dependent manner (Figure 13(A)). Furthermore, I examined the course of p38MAPK phosphorylation over time in response to sudachitin. I observed that p38MAPK phosphorylation was significantly increased at 4 h after stimulation by 100 μM sudachitin, and that this increase was sustained for up to 24 h (Figure 13(B)). As p38MAPK is phosphorylated and activated by MKK3/6, I subsequently examined whether the MKK3/6-p38MAPK cascade is activated by sudachitin. MKK3/6 phosphorylation was significantly increased following sudachitin treatment, but not following nobiletin treatment (Figure 13(C)). To confirm the involvement of p38MAPK in sudachitin-induced apoptosis, a specific p38MAPK inhibitor, SB203580, was used. As shown in Figure 13(D), SB203580 significantly reduced the sudachitin-induced phosphorylation of heat shock protein (HSP) 27, a protein that functions downstream of p38MAPK. Moreover, sudachitin-induced PARP cleavage was significantly inhibited by SB203580, indicating that sudachitin-induced apoptosis occurs through the activation of the p38MAPK pathway.

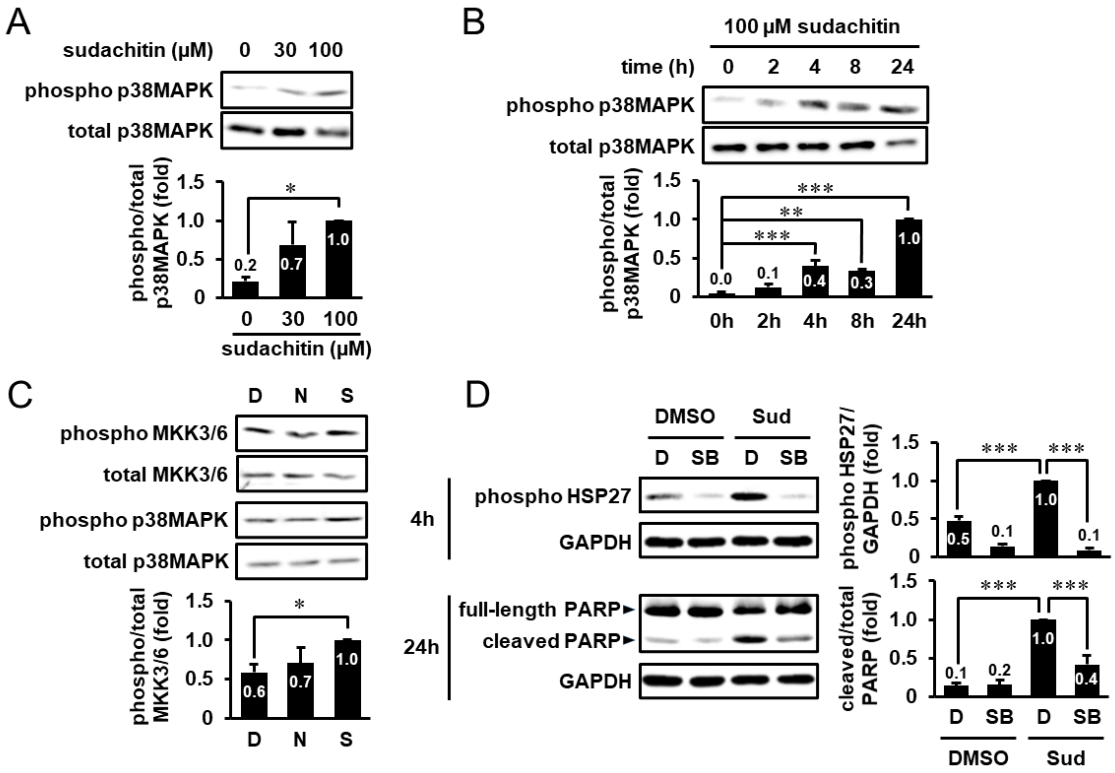

Figure 13. Sudachitin induces apoptosis through the activation of the p38MAPK pathway.

(A) HaCaT cells were treated with sudachitin (30 and 100 μM) or DMSO for 4 h. (B) HaCaT cells were stimulated with 100 μM sudachitin for indicated times. (C) HaCaT cells were stimulated with 30 μM nobiletin (N), 30 μM sudachitin (S), or DMSO (D) for 4 h. (D) HaCaT cells were treated with 30 μM sudachitin (Sud) in the presence of 10 μM SB203580 (SB) or DMSO (D) for 4 or 24 h. The cell lysates were analyzed by immunoblot analysis. The levels of phosphorylated p38MAPK, MKK3/6, HSP27, and cleaved PARP were normalized to those of total p38MAPK, MKK3/6, GAPDH, and full-length PARP, respectively. The data were expressed as the mean ± SE derived from at least three independent experiments, and statistical analysis was performed by one-way ANOVA with either Tukey's (A) or Bonferroni's (B-D) multiple comparison. ***$p < 0.001$, **$p < 0.01$, *$p < 0.05$.

3.4. Sudachitin suppresses EGF-induced ERK1/2 activation

Sudachitin, in contrast to nobiletin, induced a decrease in ERK1/2 phosphorylation (Figure 12). The activation of the ERK1/2 pathway is typically triggered by the interaction of the cell surface receptors with mitogens such as EGF, followed by the activation of Ras, Raf, MAPK/ERK kinase 1/2 (MEK1/2), and ERK1/2. In keratinocytes, EGF provides protection against UV-induced apoptosis, and the inhibitors of the epidermal growth factor receptor (EGFR) enhance UVB-induced apoptosis [59], suggesting that the EGF signaling pathway may function as a cell survival pathway. As the ERK1/2 pathway has recently attracted some attention as a potential target for the treatment of psoriasis and in anti-cancer therapy [60], I decided to further study the inhibitory effect of sudachitin on the ERK1/2 pathway. Sudachitin decreased ERK1/2 phosphorylation in a concentration-dependent manner (Figure 14(A)). ERK1/2 phosphorylation was significantly decreased at 4 and 8 h after sudachitin treatment, but returned to pretreatment levels at 24 h after treatment (Figure 14(B)). During in vitro cell culture, cells are typically cultured in FBS-supplemented media containing several growth factors such as EGF. To determine the precise effect of sudachitin on serum-induced ERK1/2 phosphorylation, serum-starved cells were stimulated with 5% FBS in the presence or absence of sudachitin. Raf-1 phosphorylation on Ser-338, required for Raf activation, and ERK1/2 phosphorylation were observed in serum-depleted cells; however, these were significantly increased in the presence of serum (Figure 14(C)). Pretreatment with sudachitin significantly inhibited the serum-stimulated activation of Raf-1 and ERK1/2. A similar result was obtained when serum-starved cells were stimulated with EGF (Figure 14(D)). I also analyzed the effect of sudachitin on EGF-stimulated ERK1/2 activation using the GAL4/Elk-1 reporter system [61]. The Elk-1 transcription factor is a downstream target of the ERK pathway. EGF stimulated an increase in the Elk-1-dependent luciferase activity, and this increase was significantly suppressed by sudachitin treatment (Figure 14(E)). These results indicate that sudachitin can inhibit EGF-stimulated ERK1/2 signaling.

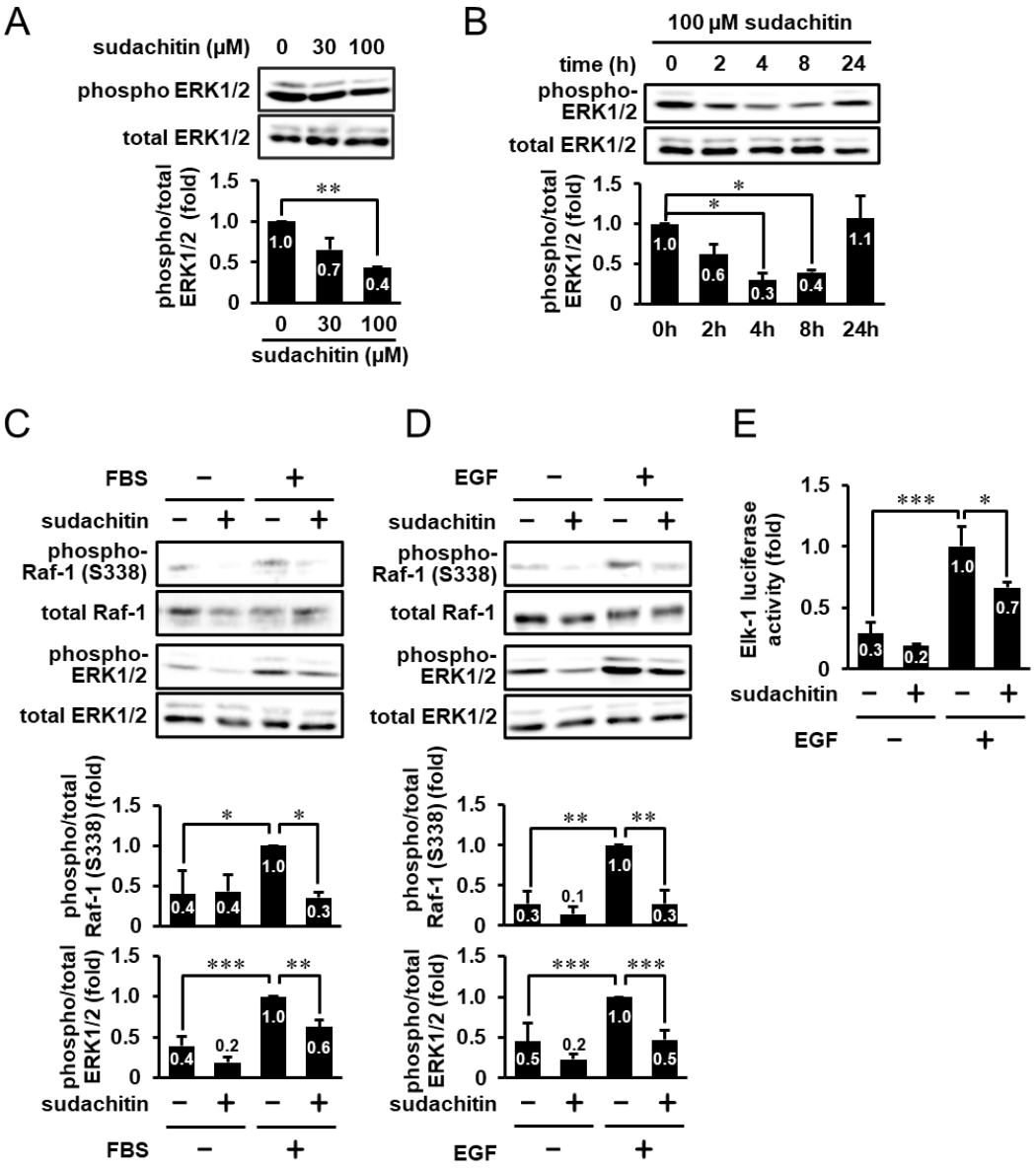

Figure 14. Sudachitin suppresses EGF-induced ERK1/2 activation.

(A) HaCaT cells were treated with sudachitin (30 and 100 μM) or DMSO for 4 h. (B) HaCaT cells were stimulated with 100 μM sudachitin for indicated times. (C and D) HaCaT cells were serum-starved for 2 h and pretreated with 30 μM sudachitin for 1 h. Then, cells were treated with (C) 5% FBS or (D) 1 nM EGF for 4 h. The cell lysates were subjected to the immunoblot analysis with the indicated antibodies. The levels of phosphorylated Raf-1 and ERK1/2 were normalized to those of total Raf-1 and ERK1/2, respectively. (E) HaCaT cells were transfected with a GAL4-responsive luciferase reporter plasmid and a GAL4-Elk-1 expression plasmid together with pCMV-β-gal. After serum-starvation for 2 h and subsequent treatment with 30 μM sudachitin for 1 h, cells were stimulated with 1 nM EGF for another 6 h. After harvest, luciferase and β-galactosidase activities were measured, and the luciferase activity was normalized to the β-galactosidase activity. All data are presented as the mean ± SE derived from at least three independent experiments, and statistical analysis was performed by one-way ANOVA with Bonferroni's multiple comparison. ***$p < 0.001$, **$p < 0.01$, *$p < 0.05$.

3.5. Sudachitin suppresses EGF-induced migration and proliferation

The ERK1/2 pathway plays important roles in many cellular functions, including cell proliferation, differentiation, migration, senescence, and apoptosis. In HaCaT cells, EGF-induced ERK1/2 activation has been shown to be associated with cell migration and proliferation [62, 63]. Therefore, I tested whether sudachitin could inhibit EGF-induced migration using the wound healing assay. The assay revealed that sudachitin significantly reduced the EGF-stimulated cell migration of HaCaT cells (Figure 15(A)). Furthermore, the effect of sudachitin on HaCaT cell proliferation was evaluated using BrdU incorporation assay. EGF stimulation caused a significant increase in HaCaT cell proliferation, and this was significantly inhibited by pretreatment with sudachitin (Figure 15(B)). These results suggest that sudachitin can inhibit HaCaT cell migration and proliferation through the inhibition of the ERK1/2 pathway.

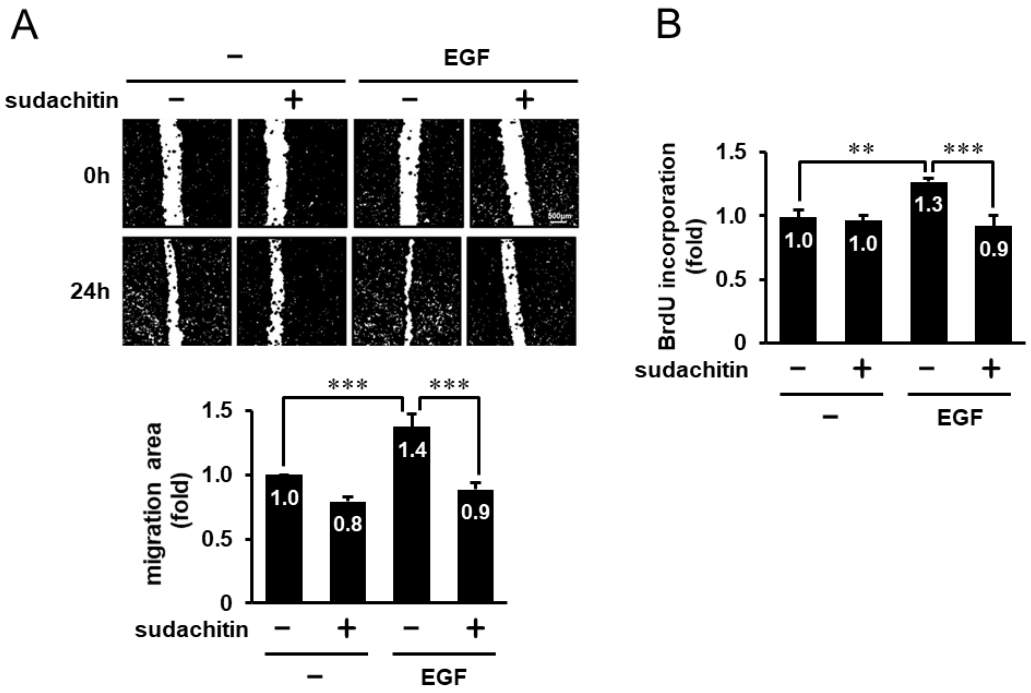

Figure 15. Sudachitin suppresses EGF-induced migration and proliferation of HaCaT cells.

(A) Serum-starved HaCaT cells were pretreated with 30 μM sudachitin in the presence of 10 μg/ml mitomycin C for 1 h, and then subjected to the in vitro wound healing assay in the presence or absence of 1 nM EGF. Images were obtained using an IN Cell Analyzer 6000 system, and wound area was quantified using ImageJ software. The migration area was calculated as the area covered by the cells after incubation for 24 h. (B) Serum-starved HaCaT cells were pretreated with 10 μM sudachitin for 1 h, and then treated with 1 nM EGF. After 24 h, cells were subjected to the BrdU incorporation assay. The data were expressed as the mean ± SE derived from at least three independent experiments, and statistical analysis was performed by one-way ANOVA with Bonferroni's multiple comparison. ***$p < 0.001$, **$p < 0.01$.

4. Discussion

The MAPK pathways are involved in many cellular responses, such as apoptosis, cell proliferation, differentiation, migration, and inflammation, and are regulated by various compounds, including flavonoids. The present study demonstrated that sudachitin can activate the p38MAPK pathway and inhibit the ERK1/2 pathway in HaCaT cells. In contrast, nobiletin, which has methoxy groups instead of hydroxyl groups at the C-5, C-7, and C-4' positions in sudachitin, activated ERK1/2. A previous study has reported that nobiletin activates ERK1/2 in rat pheochromocytoma PC12D cells [64]. Contrary to these, it has been shown that in human osteosarcoma U2OS and HOS cells, nobiletin suppressed both ERK1/2 and JNK activities [65]. These data suggest that the regulation of MAPK pathways by PMFs may be cell type-specific. A study on the structure-activity relationships of nobiletin and its analogs showed that nobiletin most potently activated ERK1/2, and that other compounds, such as tangeretin (5,6,7,8,4'-pentamethoxyflavone) and 6-demethoxynobiletin (6-hydroxy-5,7,8,3',4'-hexamethoxyflavone), were also able to activate ERK1/2 [64]. However, 5-demethylnobiletin (5-hydroxy-6,7,8,3',4'-hexamethoxyflavone), sinensetin (5,6,7,3',4'-pentamethoxyflavone), and 6-demethoxytangeretin (6-hydroxy-5,7,8,4'-pentamethoxyflavone) had no effect at a dose of 100 μM, suggesting that the methoxy substituents at the C-5, C-6, C-8, and C-3' positions are critical for activating the ERK1/2 pathway. Based on the findings of the present study, I suggest that introducing a methoxy group at the C-5 position is important for ERK1/2 activation, and that hydroxyl groups at the C-7 and C-4' positions lead to the inhibition of ERK1/2 activity. Further investigation regarding the structure-activity relationship of other PMFs is necessary to further clarify the regulation of MAPK pathways by PMFs.

I demonstrated that sudachitin induced apoptosis and inhibited EGF-induced HaCaT cell migration and proliferation. HaCaT cells are immortalized keratinocytes that retain their differentiation ability, and are widely used as an in vitro model system to study not only

keratinocyte proliferation and differentiation but also skin diseases such as psoriasis [66]. Psoriasis is a chronic inflammatory skin disease that leads to pain, itching, and bleeding in patients; it is caused by excessive cell proliferation, angiogenesis, inflammation, altered apoptotic ability, and the promotion of migration in keratinocytes [67, 68]. The induction of apoptosis and inhibition of cell migration and proliferation in keratinocytes may be ideal mechanisms to target for the treatment of psoriasis. Recently, treatment for psoriasis based on the antiproliferative and apoptotic activities of natural compounds have gained some attention [69]. A recent study showed that the EGFR and its ligands (transforming growth factor (TGF) -α, amphiregulin, and heparin-binding-EGF are overexpressed in the epidermis of active psoriatic lesions [70]. Furthermore, it has been reported that serum EGF levels are elevated in patients with psoriasis and that these correlate with disease severity [71]. As the induction of apoptosis and the suppression of EGF-induced cell migration and proliferation of keratinocytes are important for the treatment of psoriasis, sudachitin may be a potential choice to search for more effective treatments for psoriasis and other skin diseases.

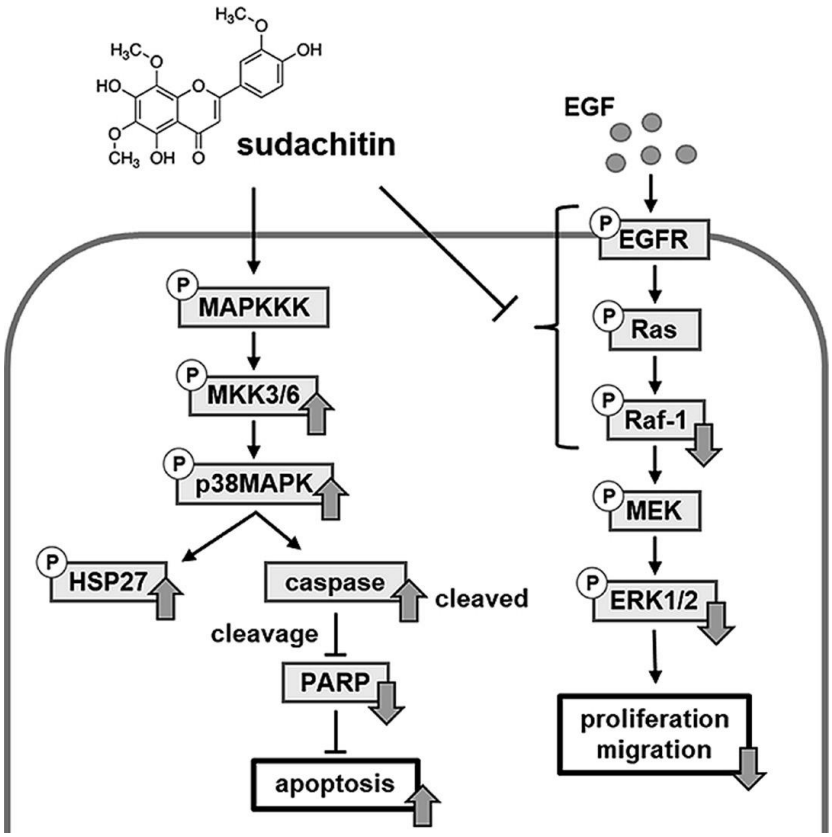

Figure 16. sudachitin induces apoptosis through activation of the p38MAPK pathway and suppresses cell proliferation through inhibition of the ERK pathway.

Chapter 4 *C. sudachi* peel extract suppresses cell proliferation

1. Introduction

The citrus peel waste of the juice extraction process contains phytochemicals such as vitamins, minerals, flavonoids, coumarin, limonoids, carotenoids, and pectin, which possess a variety of biological functions including antioxidant, anti-inflammatory, antimutagenic, anticarcinogenic, and anti-aging properties [12]. Therefore, it has potential for use in the food, cosmetic, and pharmaceutical industries. Since the peel of *C. sudachi* also contains many phenolic compounds, such as hesperidin, naringin, narirutin, and sudachitin (Table 1), which have anti-inflammatory and antioxidant properties [15, 16], it is expected that the extract of *C. sudachi* peel has various beneficial physiological properties. Recently, it was reported that the extracts of *C. sudachi* peel attenuate body weight gain in mice fed a high-fat diet and improve lipid metabolism [17, 18]. However, the effect of *C. sudachi* peel extract on skin has not been investigated. In chapter 4, I determined the effect of *C. sudachi* peel extract (SPE) on keratinocyte proliferation and differentiation.

Table 1. Contents of polyphenolic compounds in the extract of *C. sudachi* peel.

Compound	Concentration in Aqueous Extract (μM)	Concentration of SPE Containing 30% BG (μM)	Concentration in 3% SPE (μM)
hesperidin	426	298	8.95
naringin	279	195	5.85
narirutin	286	200	6.01
sudachitin	22	15	0.46

2. Materials and methods

2.1. Materials

Human EGF (Peptide Institute) and human TNF-α (Roche Diagnostics GmbH) were dissolved in PBS. Hesperidin, naringin, narirutin (Cayman Chemical Company), and sudachitin (FUJIFILM Wako Pure Chemical Corporation) were dissolved in 100% DMSO and added to the cell culture medium at a final concentration of 0.1% DMSO.

2.2. Preparation of Aqueous Extract of *C. sudachi* Peel

First, 15 g of crushed *C. sudachi* peel was immersed into 135 mL of distilled water at room temperature for 1 h. The extract was filtered through a 0.45 μm filter, and 1,3-butylene glycol (BG) was added to make a final concentration of 30%, which was designated as the SPE. The total polyphenol content of SPE was determined using the Folin-Ciocalteu method with gallic acid as a standard, and the content was 2.6 mM gallic acid equivalent. In experiments using SPE, a 30% BG solution in water was used as a negative control.

2.3. Phenolic compound evaluation by HPLC

The aqueous extract of *C. sudachi* peel was mixed with a methanol/DMSO (1:1, v/v) solution followed by 3 N HCl. After incubation at 70 °C for 1 h, the mixture was filtered through a 0.45 μm membrane filter and analyzed by reverse-phase high-performance liquid chromatography (HPLC) (Wakosil-5C18RS, 4.6 × 250 mm) (FUJIFILM Wako Pure Chemical Corporation). The elution solvents used were (A) acetonitrile/50 mM sodium dihydrogen phosphate (pH 2.3) (12:88, v/v) and (B) acetonitrile/50 mM sodium dihydrogen phosphate (pH 2.3) (60:40, v/v). Gradient elution was carried out as follows: 0-5 min 100% A, 5-21 min linear gradient to 40% B, 21-23 min 40% B, 23-45 min linear gradient to 100% B, 45-64 min 100% B, and 65-70 min linear gradient back to 100% A (initial conditions). The column temperature was 40 °C, the flow rate was 1.0 mL/min, and the

injection volume was 10 µL. The phenolic compounds were identified by the retention time and ultraviolet (UV) spectra of a standard measured from the peak area at 340 nm (Table 1 and Figure 17).

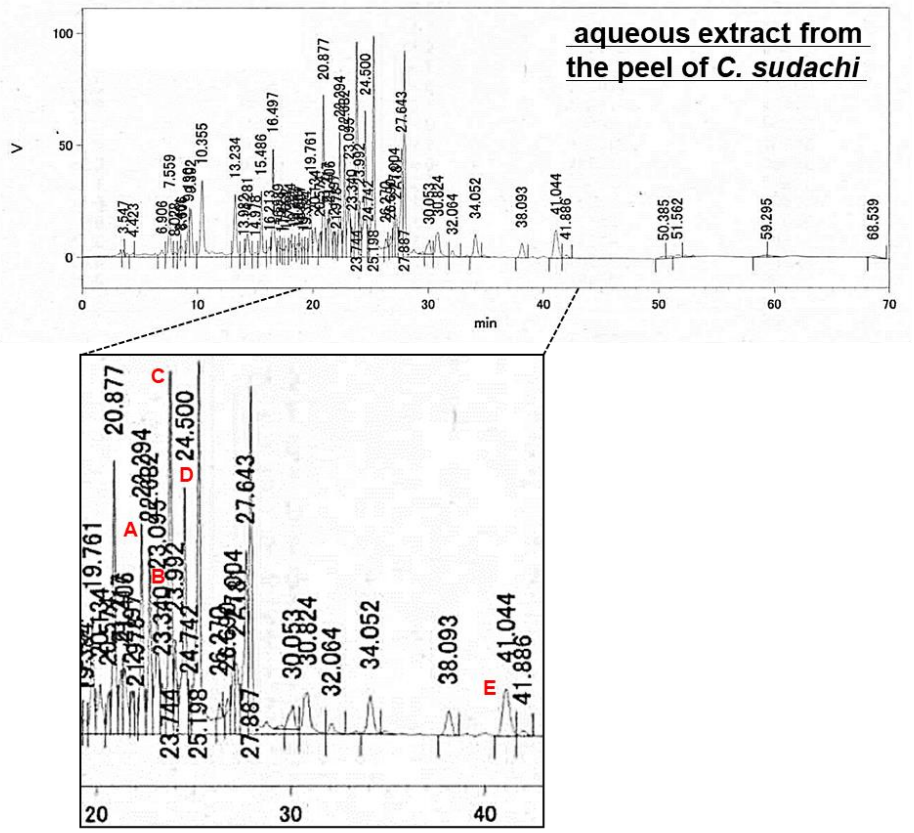

standard compound	retention time (min)	area	HPLC peak	retention time (min)	area
narirutin (1.72 mM)	22.245	3385838	A (narirutin)	22.294	562362
naringin (1.72 mM)	23.065	2932094	B (naringin)	23.095	474515
hesperidin (1.64 mM)	23.782	3665679	C (hesperidin)	23.744	953614
neohesperidin (1.64 mM)	24.470	3534963	D (neohesperidin)	24.500	824369
sudachitin (2.78 mM)	41.113	39898784	E (sudachitin)	41.044	317713

Figure 17. HPLC chromatogram of the aqueous extract from *C. sudachi* peel.

The phenolic compounds were identified by direct comparison of their UV spectra and retention times measured from the peak at 340 nm with the standard compounds.

2.4. Cell culture and induction of differentiation

HaCaT cells, from an immortalized human keratinocyte cell line developed by the German Cancer Research Center (Deutsches Krebsfors-chungszentrum, DKFZ) [43], were cultured in DMEM (FUJIFILM Wako Pure Chemical Corporation) supplemented with 10% FBS (MP Biomedicals), 100 units/mL penicillin, and 100 μg/mL streptomycin at 37 °C in a humidified incubator with 5% CO_2. Primary normal human epidermal keratinocytes (NHEKs) were purchased from PromoCell. The cells were cultured in keratinocyte growth medium 2 (PromoCell) supplemented with 100 units/mL penicillin, 100 μg/mL streptomycin, and supplement mix (PromoCell) including 0.004 mL/mL bovine pituitary extract, 0.125 ng/mL epidermal growth factor, and 0.06 mM $CaCl_2$ at 37 °C in a humidified incubator with 5% CO_2. To induce differentiation, HaCaT cells and NHEKs were cultured in calcium-free DMEM (Nacalai Tesque) and keratinocyte growth medium 2 containing 0.06 mM $CaCl_2$, respectively, and they were treated with 2 mM $CaCl_2$ for 24 h or 72 h.

2.5. Lactate dehydrogenase (LDH) assay

The activity of LDH released from the cells to the medium was measured using a Cytotoxicity LDH assay Kit-WST (Dojindo Laboratories Company Limited) according to the manufacturer's protocol. In brief, HaCaT cells were plated on a 96-well plate and were treated with 0%, 1%, 3%, and 5% SPE for 24 h. As a positive control for strong cytotoxic activity, lysis buffer was added. Working solution was added to each well, and the cells were cultured for 30 min at room temperature in the dark. After adding the stop solution, the absorbance at 490 nm was measured using the Infinite M200 plate reader (TECAN Japan).

2.6. BrdU proliferation assay

BrdU proliferation assay was performed as described in chapter 3. HaCaT cells were plated on a 96-well plate and were serum-starved for 24 h. Next, the cells were pretreated with 3% SPE for 1 h and were treated with either 3% FBS or 1 nM EGF (diluted with DMEM including 0.5% FBS) for 24 h. For NHEKs, cells were plated on a 96-well plate. After 48 h, the cells were treated with 3% SPE in keratinocyte growth medium 2 supplemented with supplement mix containing growth factor for 44 h. These treated cells were incubated with BrdU for 2 h. Following incubation with anti-BrdU antibody conjugated with peroxidase and substrate, the absorbance at 450 nm (540 nm as a reference) was measured using the plate reader.

2.7. *In vitro* wound healing assay

Immunoblot analysis was performed as described in chapter 3. HaCaT cells were seeded on a 24-well plate. After cells were grown to confluence, the culture medium was replaced with serum-free medium for 2 h. Then, cells were pretreated with BG or 3% SPE in the presence of 10 μg/ml mitomycin C. After 1 h, the confluent monolayers were scratched with a yellow pipette tip. The detached cells were removed by washing with PBS three times. Subsequently, cells were treated with BG or 3% SPE in the presence or absence of 1 nM EGF for 24 h. Images were captured in the same position at 0 and 24 h after the scratch using an IN Cell Analyzer 6000 system (GE Healthcare), and the wound areas were quantified using ImageJ software. The migration area was calculated as the difference between the initial and final wound area.

2.8. Immunoblot analysis

Immunoblot analysis was performed as described in chapter 2. Total cell lysates were prepared and subjected to immunoblot analysis using the following antibodies: anti-ERK1/2, anti-phospho-ERK1/2, anti-MEK1/2, anti-phospho-MEK1/2, anti-phospho-Raf-1 (Ser-338), anti-EGFR, anti-

phospho-EGFR (Tyr-1068) (Cell Signaling Technology), anti-Raf-1 (BD Transduction Laboratories, BD Biosciences), or anti-involucrin (Santa Cruz Biotechnology). The luminescent signals were analyzed using an LAS-4000 image analyzer (Fuji Film Company). Immunoblot band intensities were quantified using ImageJ software (NIH).

2.9. Luciferase reporter assay

Luciferase reporter assay was performed as described in chapter 3. HaCaT cells were plated in a 24-well plate, and were transfected with pFR-Luc, pFA2-Elk1, and pCMV-β-gal using FuGENE HD (Roche) according to the manufacturer's instructions. After serum-starvation for 2 h and subsequent treatment with BG or 3% SPE for 1 h, cells were stimulated with 1 nM EGF for an additional 6 h. After harvest, luciferase and *β*-galactosidase activities were measured using the Promega's luciferase system and *o*-nitrophenyl-*β*-*D*-galactopyranoside, respectively. Luciferase activity was normalized to β-galactosidase activity.

2.10. Gene expression analysis by quantitative RT-PCR

Total RNA was isolated from HaCaT cells and NHEKs using ISOGEN II (Nippon Gene Company) and then reverse-transcribed using ReverTra Ace qPCR RT Master Mix with gDNA Remover (Toyobo). Synthesized complementary DNA (cDNA) was analyzed by quantitative real-time polymerase chain reaction (RT-PCR) using StepOnePlus Real-Time PCR Systems (Applied Biosystems) with THUNDERBIRD SYBR qPCR Mix (Toyobo). The sequences of the primers used are shown in Table 2. GAPDH was used as an internal control.

Table 2. The list of primers for RT-PCR.

Gene	Forward Primer (5’ to 3’)	Reverse Primer (5’ to 3’)
keratin 1	ATATGGGGGTGGTTATGGTCC	GTGACTTGATTTGCTCCCTTTCT
keratin 10	TTGCTGAACAAAACCGCAAAG	GCCAGTTGGGACTGTAGTTCT
involucrin	ACTGAGGGCAGGGGAGAG	TCTGCCTCAGCCTTACTGTG
GAPDH	CAGCCTCAAGATCATCAGCA	CATCCACAGTCTTCTGGGTG

2.11. Statistical analysis

All experiments were performed multiple times to confirm their reproducibility. One representative set of data is shown in each figure. Data were expressed as the mean ± SE (SE), and statistical analysis was performed by Student’s t-test or one-way ANOVA followed by Bonferroni’s multiple comparisons tests using GraphPad Prism software (GraphPad Software).

3. Results

3.1. Toxicity evaluation of SPE on HaCaT cells

I first examined the cytotoxicity of SPE against human keratinocyte HaCaT cells. The cells were treated with different concentrations of SPE (0%, 1%, 3%, or 5%) for 24 h and then subjected to an LDH leakage assay. As shown in Figure 18, SPE showed no cytotoxicity at concentrations ≤3% and only very slight cytotoxicity at 5%. Because SPE showed higher antiproliferation activity without cytotoxicity at 3%, I designated 3% as the maximum tolerated concentration for the subsequent experiments.

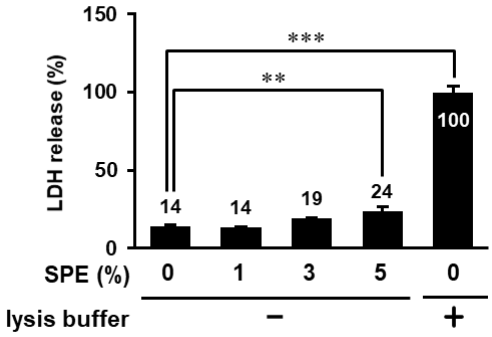

Figure 18. Cytotoxicity activity of SPE on keratinocytes.

HaCaT cells were treated with 0%, 1%, 3%, and 5% SPE for 24 h and subsequently subjected to the LDH release assay. The lysis buffer was added as a positive control. The data were expressed as the mean ± SE derived from at least three independent experiments, and statistical analysis was performed by one-way ANOVA with Bonferroni's multiple comparisons test. *** $p < 0.001$, ** $p < 0.01$.

3.2. SPE suppresses cell proliferation and cell migration

Next, I evaluated the effect of SPE on cell proliferation in HaCaT cells using the BrdU incorporation assay. The proliferation of serum-stimulated HaCaT cells was significantly suppressed by SPE (1% and 3%) treatment in a concentration-dependent manner (Figure 19(A)), suggesting that SPE could suppress cell proliferation of HaCaT cells. I attempted to elucidate the detailed effect of SPE on cell proliferation in HaCaT cells using the BrdU incorporation assay. In keratinocytes, the family of EGF, such as EGF and TGF-α, promotes cell proliferation,

differentiation, and migration, while it inhibits apoptosis through binding of the EGFR, which is a receptor tyrosine kinase [72]. Hence, I examined whether SPE suppresses EGF-induced cell proliferation of HaCaT cells. The BrdU incorporation assay showed that SPE could significantly attenuate EGF-induced cell proliferation of HaCaT cells (Figure 19(B)). Furthermore, the *in vitro* wound healing assay indicated that EGF-stimulated cell migration was also significantly inhibited by pretreatment with 3% SPE in HaCaT cells (Figure 19(C)).

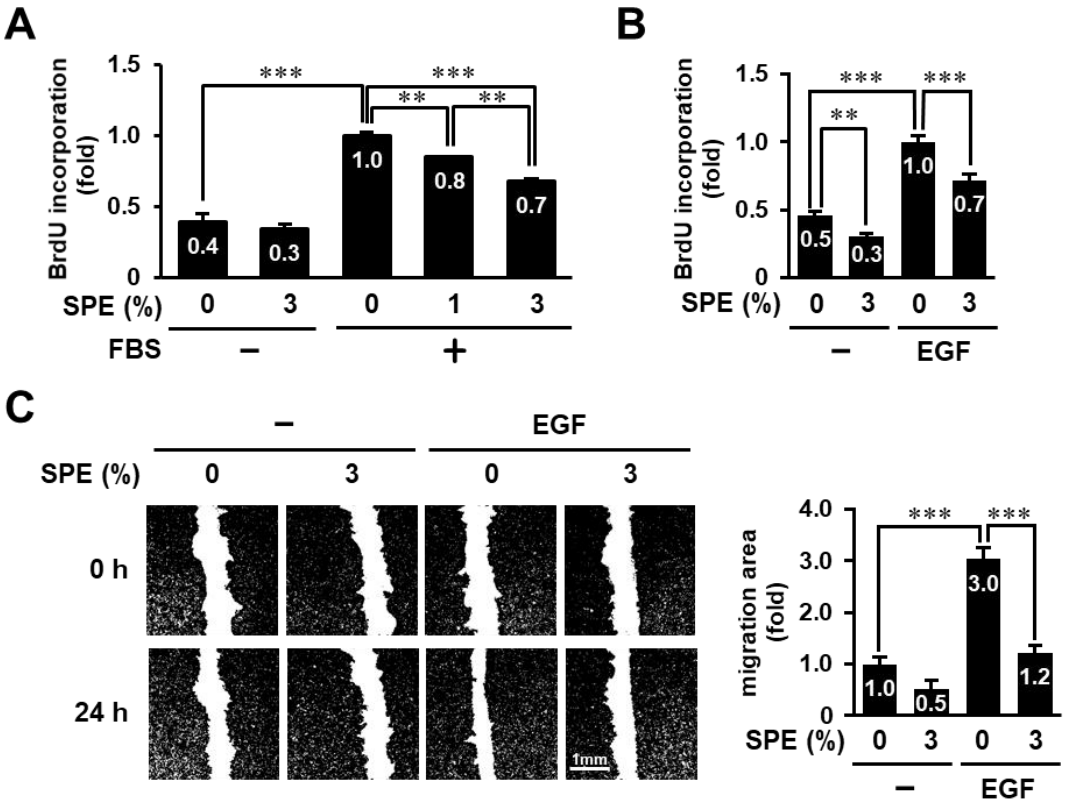

Figure 19. SPE suppresses EGF-induced proliferation and migration of HaCaT cells.

(A) Serum-starved HaCaT cells were pretreated with 0%, 1%, and 3% SPE for 1 h, and then incubated in the presence or absence of 3% FBS. (B) Serum-starved HaCaT cells were pretreated with 3% SPE for 1 h and subsequently incubated in the presence or absence of 1 nM EGF. After 24 h, the cells were subjected to the BrdU incorporation assay. (A and B) After 24 h, the cells were subjected to BrdU incorporation assay. (C) Serum-starved HaCaT cells were pretreated with BG or 3% SPE in the presence of 10 μg/ml mitomycin C for 1 h, and then subjected to the *in vitro* wound healing assay in the presence or absence of 1 nM EGF. Images were obtained using an IN Cell Analyzer 6000 system, and wound area was quantified using ImageJ software. The migration area was calculated as the area covered by the cells after incubation for 24 h. The data were expressed as the mean ± SE derived from at least three independent experiments, and statistical analysis was performed by one-way ANOVA with Bonferroni's multiple comparisons test. *** $p < 0.001$, ** $p < 0.01$.

3.3. SPE suppresses cell proliferation and the EGFR-ERK Pathway

Cell proliferation is regulated by complex signaling networks, including the MAPK signaling pathway. Activation of the ERK pathway is triggered by the binding of the growth factor to its receptor(s) and is involved in various cellular functions. The ERK signaling pathway involves the sequential activation of Ras, Raf-1, MEK1/2, and ERK1/2. Therefore, I assessed whether SPE suppresses the activation of the ERK pathway, including Raf-1, MEK1/2, and ERK1/2. As shown in Figure 20(A), SPE significantly suppressed EGF-induced phosphorylation of Raf-1, MEK1/2, and ERK1/2. A similar result was obtained when using serum as a stimulator instead of EGF (data not shown). In response to the binding of EGF to EGFR, EGFR dimerizes and autophosphorylates at several tyrosine residues, including Tyr-1068, leading to the activation of a network of signaling pathways [72]. Therefore, I examined whether SPE could inhibit EGF-induced EGFR phosphorylation at Tyr-1068. EGF increased EGFR phosphorylation at Tyr-1068, and pretreatment with 3% SPE significantly suppressed EGFR phosphorylation, as well as ERK activation (Figure 20(A)). Furthermore, I examined the effect of SPE on the activity of Elk-1, a downstream transcription factor of the ERK pathway. The activity of Elk-1 reporter was increased by EGF stimulation, and this increase was significantly inhibited by 3% SPE treatment (Figure 20(B)). These results suggest that SPE can suppress keratinocyte proliferation through inhibition of the EGF-EGFR-ERK signaling pathway.

Although SPE suppressed EGFR phosphorylation on Tyr-1068, the inhibitory efficiency (23%) was less than the efficiency on Raf-1, MEK1/2, and ERK1/2 phosphorylation (41-54%), suggesting that SPE may exert an inhibitory effect through multiple targets (EGF-EGFR and its downstream molecules). Thus, in order to narrow down the target candidates of SPE, I examined the effect of SPE on TNF-α-induced EGFR-independent ERK1/2 activation. As shown in Figure 20(C), TNF-α did not affect the phosphorylation of EGFR at Tyr-1068. On the other hand, ERK1/2 was

significantly activated in response to TNF-α, and 3% SPE almost completely inhibited this increase.

These results indicate that SPE can suppress both EGFR and its downstream molecule(s).

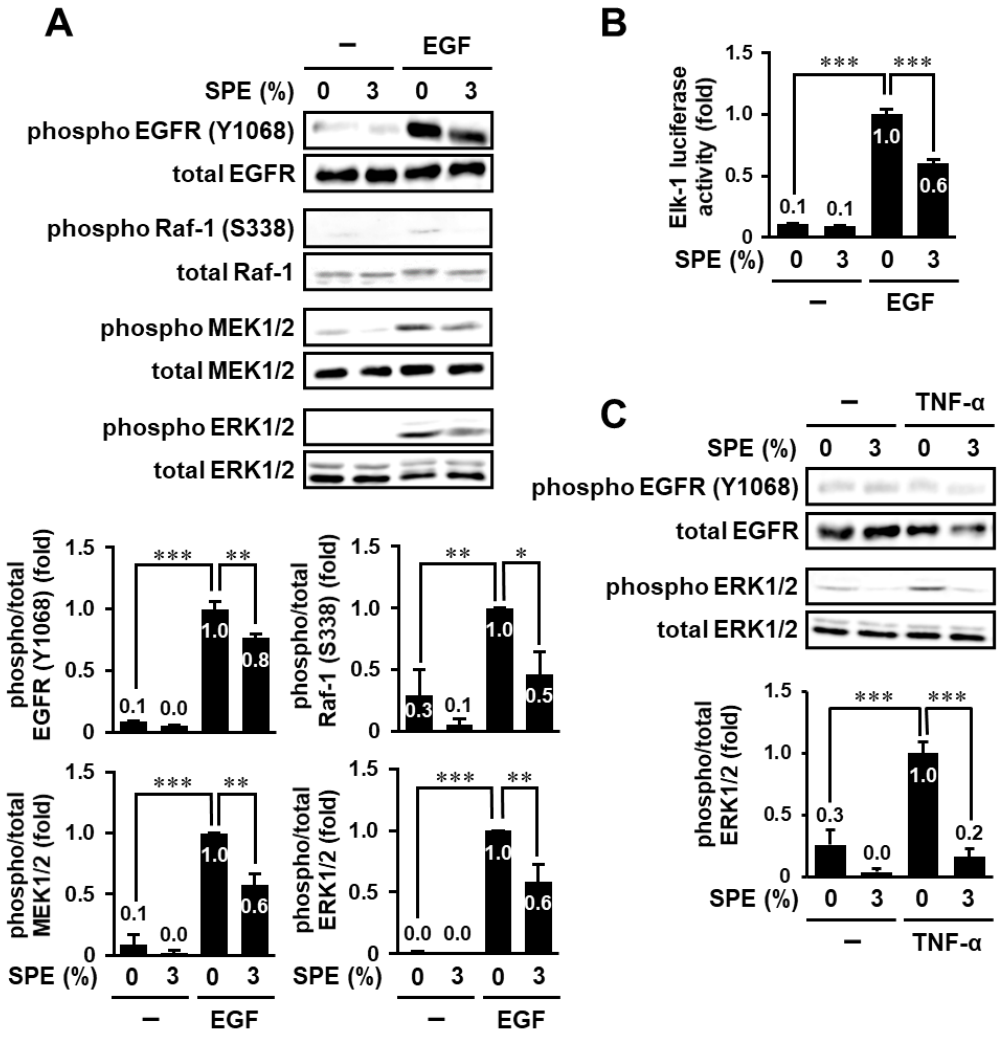

Figure 20. SPE inhibits EGF-induced the EGFR-ERK pathway in HaCaT cells.

(A) HaCaT cells were serum-starved for 2 h and were treated with 3% SPE for 1 h. Then, the cells were stimulated with 1 nM EGF for 1 h. The cell lysates were analyzed by immunoblot analysis. The levels of phosphorylated proteins were normalized to those of total proteins. (B) HaCaT cells were transfected with a GAL4-responsive luciferase reporter plasmid and GAL4-Elk-1 expression plasmid together with pCMV-β-gal. The transfected cells were serum-starved for 2 h and subsequently treated with 3% SPE for 1 h. Then, the cells were stimulated with 1 nM EGF for 6 h and subjected to the luciferase reporter assay. The luciferase activity was normalized to the β-galactosidase activity. (C) HaCaT cells were serum-starved for 2 h and were treated with 3% SPE for 1 h. Then, the cells were stimulated with 10 ng/mL TNF-α for 1 h. The cell lysates were analyzed by immunoblot analysis. The levels of phosphorylated proteins were normalized to those of total proteins. The data are expressed as the mean ± SE derived from at least three independent experiments, and statistical analysis was performed by one-way ANOVA with Bonferroni's multiple comparisons test. *** $p < 0.001$, ** $p < 0.01$, * $p < 0.05$.

3.4. SPE suppresses cell proliferation and ERK activity in NHEKs

Next, I determined the effect of SPE on cell proliferation and ERK1/2 activation in not only an immortalized human keratinocyte cell line, HaCaT, but also primary NHEKs. As shown in Figure 21(A), the BrdU incorporation assay showed that SPE could significantly attenuate cell proliferation of NHEKs. Similarly, SPE significantly inhibited ERK1/2 phosphorylation in NEHKs (Figure 21(B)). These data suggest that SPE can also inhibit cell proliferation and ERK1/2 activation in primary normal keratinocytes.

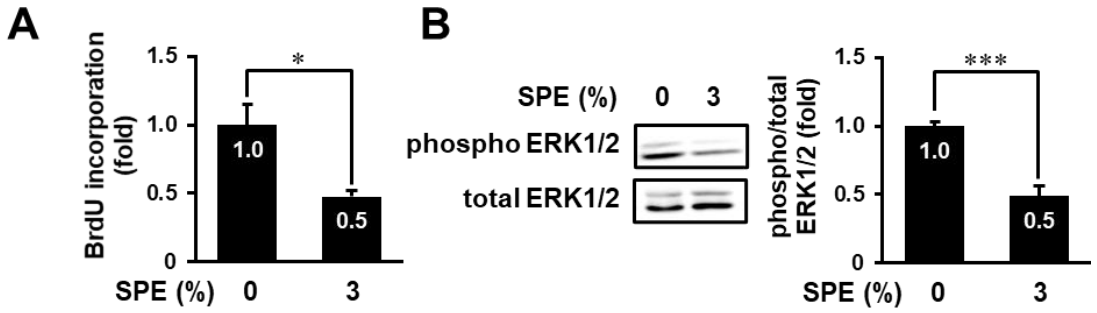

Figure 21. SPE inhibits cell proliferation and ERK1/2 in NHEKs.

(A) NHEKs were treated with 3% SPE for 44 h and were subjected to the BrdU incorporation assay. (B) NHEKs were treated with 3% SPE for 1 h. Then, the cell lysates were prepared and immunoblotted with anti-ERK1/2 and anti-phospho-ERK1/2 antibodies. The levels of phosphorylated ERK1/2 were normalized to the levels of the total ERK1/2. The data are expressed as the mean ± SE derived from at least three independent experiments, and statistical analysis was performed by Student's t-test. *** $p < 0.001$, * $p < 0.05$.

3.5. Search for biologically active compound(s) in SPE

I previously reported that sudachitin, a PMF isolated from the peel of *C. sudachi*, suppressed proliferation and induced apoptosis of HaCaT cells at 30 μM (chapter 3). Thus, I examined whether sudachitin could suppress keratinocyte proliferation at a concentration in 3% SPE (0.46 μM, Table 1). Although 3% SPE significantly inhibited serum-stimulated proliferation of HaCaT cells, sudachitin showed no inhibition of growth even at a higher concentration (1 μM) (Figure 22(A)). However, in a concentration of 30 μM, it inhibited proliferation, consistent with a result in chapter 3.

In chapter 3, I reported that sudachitin at 30 μM also suppressed the ERK pathway in HaCaT cells. Because the peel of *C. sudachi* contains many phenolic compounds, including hesperidin, naringin, narirutin, and sudachitin (Table 1), I attempted to identify active compound(s) that could affect the ERK pathway in keratinocytes. Although SPE (1-3%) inhibited ERK1/2 phosphorylation in a concentration-dependent manner, hesperidin (10 μM), naringin (10 μM), narirutin (10 μM), or sudachitin (1 μM) individually had no effect on phosphorylation of ERK1/2 even at higher concentrations than those in SPE (Figure 22(B)). Furthermore, I also examined whether hesperetin (hesperidin aglycone) and naringenin (aglycone of naringin and narirutin) affect ERK1/2 activity, because aglycones generally show a higher permeability than glycosides [73]. However, these aglycones, like their glycosides, had no inhibitory effect (Figure 22(B)). Additionally, as shown in Figure 22(C), these phenolic compounds, except for sudachitin, failed to suppress ERK1/2 phosphorylation even at high concentration (100 μM). These results suggest that some known natural products, including hesperidin, naringin, and sudachitin, and/or unidentified compound(s) might additively or synergistically contribute to antiproliferation and inhibitory activity against ERK signaling in keratinocytes.

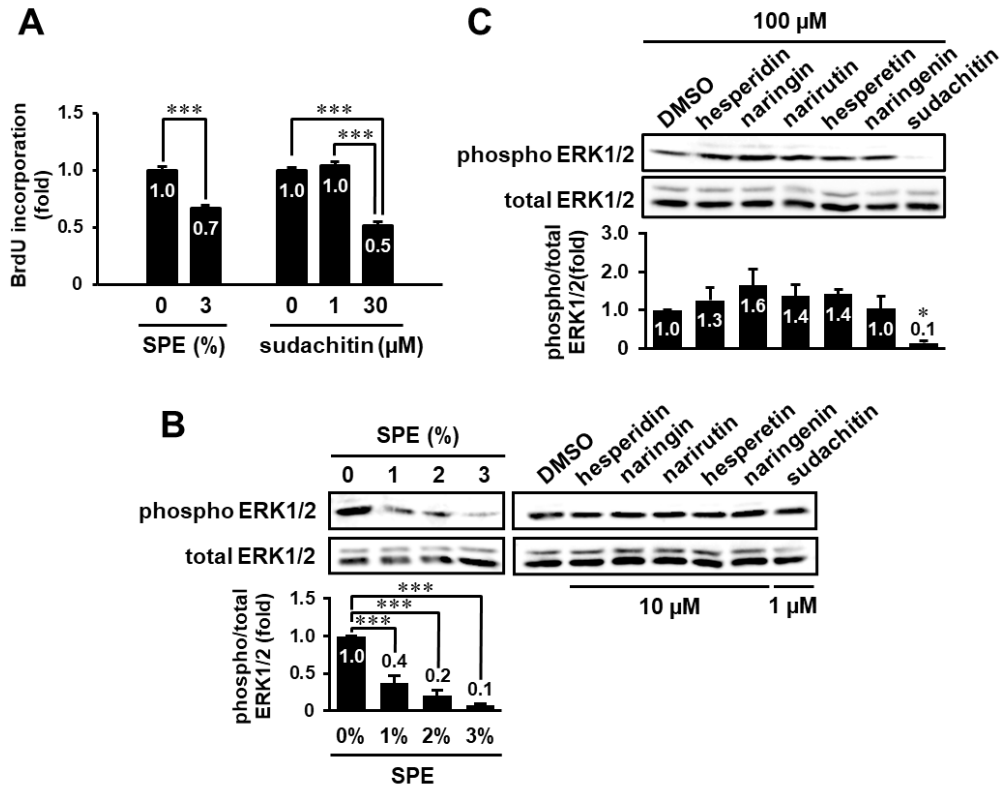

Figure 22. Effects of some phenolic compounds in the extract of *C. sudachi* peels on cell proliferation and ERK1/2 phosphorylation

(A) Serum-starved HaCaT cells were pretreated with SPE (3%) or sudachitin (1 or 30 μM) for 1 h and subsequently incubated in the presence of 3% FBS. After 24 h, the cells were subjected to a BrdU incorporation assay. (B) HaCaT cells were treated with either 0-3% SPE, DMSO, 10 μM hesperidin, 10 μM naringin, 10 μM narirutin, 10 μM hesperetin, 10 μM naringenin, or 1 μM sudachitin for 1 h. (C) HaCaT cells were treated with 100 μM hesperidin, 100 μM naringin, 100 μM narirutin, 100 μM hesperetin, 100 μM naringenin, or 100 μM sudachitin for 1 h. (B and C) Then, the cell lysates were prepared and immunoblotted with anti-ERK1/2 and anti-phospho-ERK1/2 antibodies. The levels of phosphorylated ERK1/2 were normalized to the levels of the total ERK1/2. All experiments were performed multiple times with similar results. The data are expressed as the mean ± SE derived from at least three independent experiments, and statistical analysis was performed by one-way ANOVA with Bonferroni's multiple comparisons test. *** $p < 0.001$, * $p < 0.05$.

3.6. SPE potentiates calcium-induced keratinocyte differentiation

In addition to hyperproliferation, altered keratinocyte differentiation is also a characteristic of several skin diseases, including skin cancer and psoriasis [74]. Therefore, I examined whether SPE could also affect keratinocyte differentiation by determining the messenger RNA (mRNA) levels of keratinocyte differentiation markers (keratin 1, keratin 10, and involucrin). Since differentiation

of HaCaT cells is induced by switching from a low-to high-calcium medium [75], HaCaT cells cultured in calcium-free medium were treated with 3% SPE in the presence or absence of 2 mM $CaCl_2$. Quantitative RT-PCR analysis showed that high calcium increased the expression of keratin1, keratin10, and involucrin in HaCaT cells (Figure 23(B-D)). Although SPE did not affect in the absence of calcium, SPE significantly enhanced the increase in expression of differentiation markers elicited by high calcium. These results suggest that SPE may synergistically enhance calcium-induced keratinocyte differentiation in HaCaT cells.

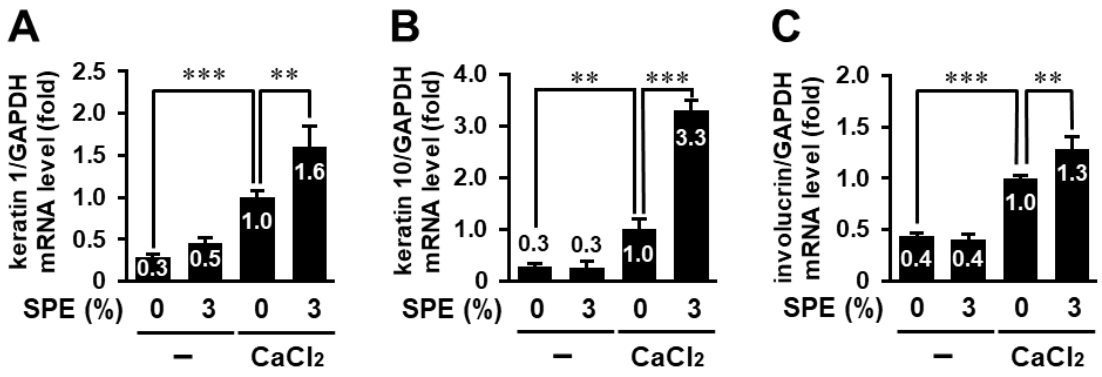

Figure 23. SPE potentiates calcium-induced keratinocyte differentiation in HaCaT cells.

(A-C) HaCaT cells cultured in calcium-free medium were treated with 2 mM $CaCl_2$ in the presence or absence of 3% SPE for 72 h. The cells were subjected to quantitative RT-PCR. The messenger RNA (mRNA) levels of keratin 1 (A), keratin 10 (B), and involucrin (C) were normalized to that of GAPDH. The data are expressed as the mean ± SE derived from at least three independent experiments, and statistical analysis was performed by one-way ANOVA with Bonferroni's multiple comparisons test. *** $p < 0.001$, ** $p < 0.01$.

3.7. SPE promotes calcium-stimulated differentiation of NHEKs

Finally, I examined the effect of SPE on the differentiation in NHEKs. Stimulation with a high concentration of Ca^{2+} (2 mM) resulted in significantly increased involucrin mRNA expression in NHEKs, and 3% SPE induced a further increase in involucrin mRNA expression (Figure 24(A)). Furthermore, I assessed the protein level of involucrin by immunoblot analysis. The expression of involucrin protein tended to be increased by calcium stimulation and was significantly increased

in combination with 3% SPE when compared to the control group (Figure 24(B)). These results strongly support that SPE can also promote calcium-induced differentiation of keratinocytes.

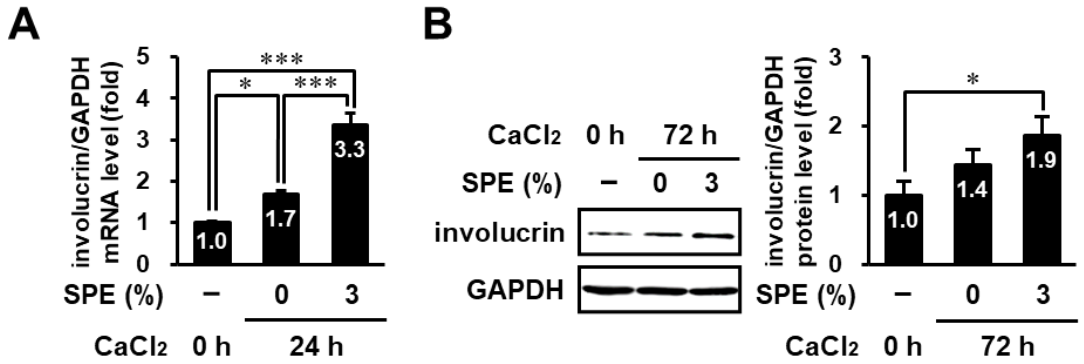

Figure 24. SPE promotes calcium-stimulated differentiation of NHEKs.

NHEKs cultured in keratinocyte growth medium 2 including 0.06 mM $CaCl_2$ were treated with 2 mM $CaCl_2$ in the presence or absence of 3% SPE for 24 h or 72 h. The cells were subjected to quantitative RT-PCR (A) and immunoblot analysis (B). The mRNA and protein levels of involucrin were normalized to those of GAPDH. The data are expressed as the mean ± SE derived from at least three independent experiments, and statistical analysis was performed by one-way ANOVA with Bonferroni's multiple comparisons test. *** $p < 0.001$, * $p < 0.05$.

4. Discussion

The ERK pathway (Ras-Raf-MEK-ERK) is involved in the regulation of various cellular processes, such as adhesion, proliferation, cell cycle progression, migration, survival, differentiation, metabolism, and transcription. Previous studies showed that many extracts exert various biological functions by modulating the ERK pathway [76, 77]. For example, carrot pentane-based fractions inhibited the proliferation of tumorigenic HaCaT cells through inhibition of the ERK and phosphatidylinositol 3-kinase-Akt pathways, and the extract of *Centella* asiatica induced keratinocyte migration through focal adhesion kinase-Akt, ERK, and p38MAPK signaling. In this study, I demonstrated that the aqueous extract of *C. sudachi* peel suppresses cell proliferation of HaCaT cells and normal keratinocytes. Furthermore, the extract of *C. sudachi* peel attenuated EGF-induced phosphorylation of EGFR, Raf-1, MEK1/2, and ERK1/2. The development of cancer drugs targeting the EGFR-Ras-Raf-MEK-ERK pathway has been attempted. EGFR tyrosine kinase inhibitors, such as gefitinib, inhibit autophosphorylation by binding to the ATP-binding pocket of the intracellular catalytic kinase domain, resulting in inhibition of the downstream signaling pathways [78]. On the contrary, epigallocatechin-3 gallate, a component of green tea, inhibits the binding of the ligand to EGFR and, subsequently, the dimerization and activation of EGFR [79]. The extract of *C. sudachi* peel may also bind to the ligand-binding site or ATP-binding pocket of EGFR and suppress the autophosphorylation and activation of EGFR. Moreover, the extract of *C. sudachi* peel also suppressed TNF-α-induced ERK pathway activation, although TNF-α did not affect EGFR phosphorylation on Tyr-1068. Previous studies showed that TNF-α stimulates ERK activation through EGFR-dependent or -independent pathways, and that EGFR-independent ERK activation is mediated through the activation of TGF-β-activated kinase 1 and tumor progression locus 2 [80, 81, 82]. Taken together, the extract of *C. sudachi* peel may attenuate EGF-induced ERK activation through inhibition of not only EGFR but also its downstream molecule(s), such as Ras and Raf-1, or other signaling molecule(s). Because the

combination of drugs targeting different proteins may often increase efficiency and attenuate toxicity [83], the extract of *C. sudachi* peel may be a potential therapeutic avenue for skin diseases caused by abnormalities in the ERK pathway.

I also demonstrated that the extract of *C. sudachi* peel could potentiate calcium-induced keratinocyte differentiation of HaCaT cells and NHEKs. Calcium is involved in the differentiation and proliferation process of keratinocytes [84]. Keratinocytes in low-calcium conditions proliferate but fail to differentiate, and exposure to high calcium levels results in keratinocyte differentiation [75]. Moreover, not only is intracellular calcium concentration a key regulator for keratinocyte differentiation but so is EGFR. EGFR is expressed in all layers of keratinocytes, especially in the basal layer, and a decrease in EGFR expression due to exit the basal layer leads to suppression of proliferation and initiation of differentiation [85]. A previous study showed that both EGFR small interfering RNA (siRNA) and EGFR inhibitors increase the expression of several differentiation markers, including keratin 1, keratin 10, and involucrin in primary human keratinocytes, intact epidermis, and skin squamous cell carcinomas [86]. Furthermore, the expression of differentiation markers was reduced by EGF treatment in a keratinocyte cell line derived from newborn rat skin [87]. Additionally, it was reported that the desmoglein-1/Erbin interaction promoted keratinocyte differentiation by attenuating ERK1/2 activity [88]. On the other hand, a previous study showed that inhibition of MEK1/2, a downstream of EGFR, blocked calcium-induced involucrin expression [35]. In this study, SPE enhanced keratinocyte differentiation only under high-calcium conditions, although SPE inhibited calcium-induced ERK1/2 activation. Therefore, I speculate that SPE may potentiate calcium-stimulated keratinocyte differentiation through the inhibition of EGFR, and further studies are needed to investigate the involvement of the ERK pathway in SPE-enhanced keratinocyte differentiation.

Abnormalities of the EGF-EGFR-ERK signaling pathway in keratinocytes cause skin disorders. For example, EGFR and its ligands are overexpressed in patients with psoriasis, and increased

serum EGF concentrations correlate with the severity of psoriasis [70, 71]. Overactivation of EGFR caused by a higher concentration of EGF increased epidermal stress and induced remarkable epidermal disorganization with the loss of proper stratification in in vitro human skin equivalents [89]. Furthermore, the ERK pathway is also recognized as an important target for the treatment of cSCC. Oncogenic Ras was shown to be involved in the growth and development of cSCC through the activation of the ERK pathway [37]. EGFR-activating mutations cause constitutive activation of the ERK pathway in cutaneous keratoacanthoma and cSCC [90]. On the other hand, it was reported that a potent Ras inhibitor, salirasib, did not exhibit antitumor activity due to the disability of signaling transmission from Ras to Raf in cSCC [91]. Moreover, mutations in Ras were caused by treating with Raf inhibitor, vemurafenib, in cSCC, and these lesions were blocked by a MEK1/2 inhibitor [92]. As the inhibition of the EGFR-ERK pathway is important for the treatment of skin disorders, such as psoriasis and cSCC, further research on mechanisms underlying the inhibition of EGFR-ERK signaling by SPE may lead to the development of therapeutic agents for more effective treatments against skin diseases characterized by abnormalities in the EGFR-ERK signaling pathway.

In this study, I demonstrated that the aqueous extract of *C. sudachi* peel suppresses ERK1/2 phosphorylation. Furthermore, I demonstrated that sudachitin, a PMF extracted from the peel of *C. sudachi*, suppresses cell proliferation and migration thorough inhibition of the ERK pathway in HaCaT cells at a relatively high concentration (30 μM) in chapter 3. Therefore, although I examined whether polyphenolic compound(s) included in *C. sudachi* peel could inhibit the ERK pathway, hesperidin, naringin, narirutin, sudachitin, hesperetin (an aglycone of hesperidin), and naringenin (an aglycone of naringin and narirutin) had no effects even at higher concentrations than those in SPE. Additionally, these phenolic compounds, except for sudachitin, failed to suppress ERK1/2 phosphorylation even at high concentration (100 μM) (Figure 22(C)), Supplementary Materials). However, previous studies reported that many flavones such as

hesperidin and naringin isolated from citrus peel suppress the ERK1/2 pathway [93, 94, 95]. For example, hesperidin (approximately 10 μM) found in C. tangerine peel suppressed lipopolysaccharide-induced ERK1/2 phosphorylation in HaCaT cells [93], and naringin (100 μM) isolated from *C. grandis* attenuated EGF-induced ERK1/2 phosphorylation in human lung adenocarcinoma cells [94]. Hesperetin also inhibited vascular endothelial growth factor-induced ERK1/2 phosphorylation at 25 μM in human umbilical vascular endothelial cells [95]. On the other hand, it was reported that hesperidin (40 μM), naringin (100 μM), and hesperetin (50 μM) facilitated ERK1/2 phosphorylation in normal human hepatic cells, human bladder carcinoma cells, and murine B16-F10 melanoma cells, respectively [96, 97, 98]. Therefore, phenolic compounds may regulate the ERK pathway in a cell type-dependent manner, and the phenolic compounds evaluated in this study may have no effect on ERK activity in keratinocytes. Other phenolic compounds contained in Citrus peels have been shown to possess ERK1/2 inhibitory activity [99, 100]. Tangeretin and quercetin, which are flavonoids obtained from Citrus peels, inhibited estradiol-induced ERK1/2 phosphorylation in human mammary ductal carcinoma and suppressed ERK1/2 phosphorylation induced by stimulation of 12-O-tetradecanoylphorbol-13-acetate in human breast carcinoma cells, respectively. Taken together with these studies, I speculate that some known natural products, including hesperidin, naringin, and sudachitin, and/or unidentified compound(s) may additively or synergistically affect keratinocyte proliferation and differentiation through regulation of the ERK1/2 pathway. Further studies are needed to identify bioactive compound(s) and investigate the underlying mechanisms of the action.

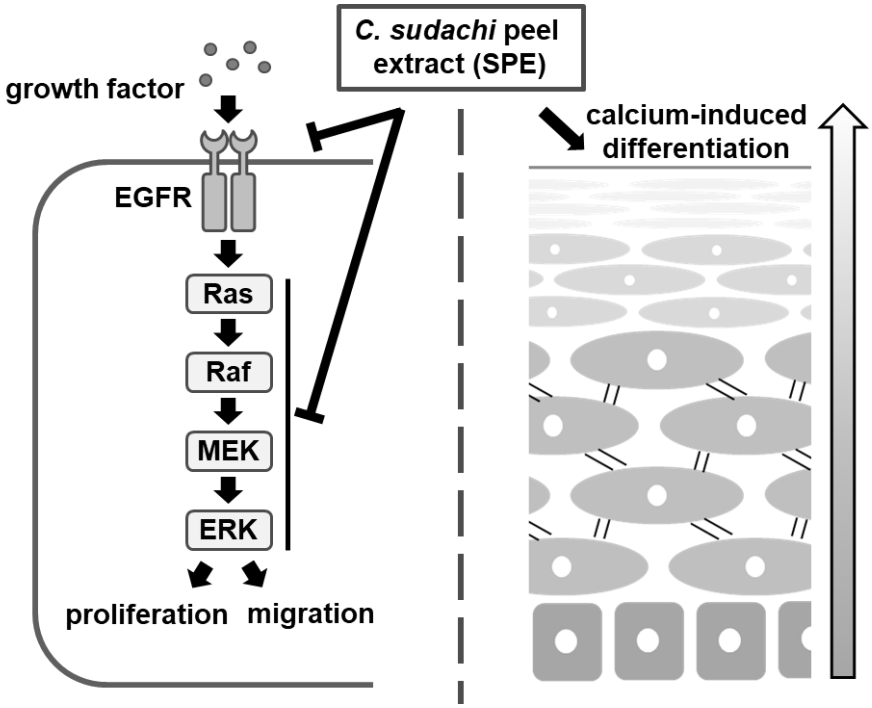

Figure 25. *C. sudachi* peel extract suppresses cell proliferation and promotes the differentiation of Keratinocytes.

Chapter 5 Conclusion

In chapter 2, I attempted to elucidate novel biological activities of sudachitin and 3'-demethoxysudachitin. I showed that two PMFs, sudachitin and nobiletin, significantly suppressed cell proliferation at 30 and 100 μM in human keratinocytes HaCaT. Although 3'-demethoxysudachitin exhibited an antiproliferative activity at a concentration of 100 μM, little effect was observed at 30 μM. Next, I examined whether these polymethoxyflavones induce apoptosis or autophagy. My results showed that sudachitin selectively induced apoptosis in human HaCaT cells, and nobiletin promoted autophagy but not apoptosis. On the other hands, 3'-demethoxysudachitin failed to induce apoptosis and autophagy. These results show three polymethoxyflavones have different effects on apoptosis and autophagy in HaCaT cells. Further studies are needed to clarify the mechanism behind sudachitin and nobiletin-induced cell death, and understanding the structure and biological activity of PMFs may lead to the discovery of potential therapeutic agents.

In chapter 3, I investigated the mechanism underlying sudachitin-induced apoptosis via the MAPK pathways. To confirm the apoptotic effect of sudachitin, I measured caspase activation in HaCaT cells. Sudachitin caused a dose-dependent proteolytic cleavage and the activation of caspase-3 and significantly decreased the level of full-length Bid, accompanied by an increased amount of its cleaved product, truncated Bid. Furthermore, sudachitin-induced PARP cleavage was prevented by pan-caspase inhibitor z-VAD-FMK. These results indicated that sudachitin induces apoptosis via the caspase pathway. Next, I also assessed whether sudachitin-induced apoptosis is associated with MAPK family. Sudachitin increased p38MAPK and JNK phosphorylation, but significantly decreased ERK1/2 phosphorylation. In contrast, nobiletin significantly increased ERK1/2 phosphorylation. To confirm the involvement of p38MAPK in sudachitin-induced apoptosis, a specific p38MAPK inhibitor, SB203580, was used. SB203580 significantly inhibited sudachitin-induced PARP cleavage, indicating that sudachitin-induced apoptosis occurs through

the activation of the p38MAPK pathway. In addition, Sudachitin suppressed Raf-1 and ERK1/2 activation by FBS and EGF treatment after serum starvation. Moreover, sudachitin inhibited EGF-promoted cell migration and proliferation. Because induction of apoptosis and suppression of EGF-induced cell migration and proliferation of keratinocytes are important for psoriasis treatment, sudachitin has therapeutic potential in skin diseases.

In chapter 4, I determined the effect of *C. sudachi* peel extract (SPE) on keratinocyte proliferation and differentiation. My data showed that SPE significantly suppressed EGF-promoted cell proliferation and cell migration. In addition, SPE significantly suppressed the phosphorylation of EGFR and Raf-1, MEK1/2, and ERK1/2 induced by EGF treatment. Furthermore, in order to narrow down the target candidates of SPE, I examined the effect of SPE on TNF-α-induced EGFR-independent ERK1/2 activation. TNF-α did not affect the phosphorylation of EGFR at Tyr-1068. On the other hand, ERK1/2 was significantly activated in response to TNF-α, and SPE almost completely inhibited this increase. These results indicate that SPE can suppress both EGFR and its downstream molecule(s). Next, I examined whether SPE could also affect keratinocyte differentiation. Quantitative RT-PCR analysis showed that SPE significantly enhanced the increase in expression of differentiation markers elicited by high calcium in HaCaT cells. SPE also possessed antiproliferation and pro-differentiation activities in primary keratinocytes. Thus, it may be effectively used for the prevention and treatment of skin diseases, such as psoriasis and cutaneous squamous cell carcinoma, caused by abnormalities in proliferation and differentiation in epidermal keratinocytes.

In summary, I demonstrated that *C. sudachi* peel extract and sudachitin have novel physiological activities such as induction of apoptosis, anti-proliferation activity and pro-differentiation activity via the mechanisms including inhibition of EGFR-ERK pathway and activation of p38MAPK pathway in keratinocytes. Therefore, *C. sudachi* peel extracts and its functional components has therapeutic potential in skin diseases.

Chapter 6 Acknowledgments

I appreciate Associate Prof. Keizo Yuasa for their support of this research project and my graduate education. I am grateful to Honorary Prof. Akihiko Tsuji for continuous encouragement. I would like to thank the member of my committee, Prof. Hideaki Nagamune, Prof. Hitoshi Matsuki, and Prof. Eiji Sakuradani for comment on this work. I also am grateful to Associate Prof. Tetsuya Akamatsu, Dr. Ichiro Yoshida, Ms. Sara Murakami, and Dr. Yusei Shinohara for advice on experimental design. In addition, I am deeply grateful to Honorary Prof. Masao Tsukayama and all staff of Research and Development Department of Matsuyama Co., Ltd. for the prepare and provide of sample, and would like to thank Dr. Yoshitaka Nii of Food and Biotechnology Division of Tokushima Prefectural Industrial Technology Center for helping me analyze the extract. I would also like to express my gratitude to Tokushima Shimbun Social and Cultural Foundation for their financial support. Finally, I thank to Ms. Saki Hirose, and Ms. Mami Nishitani, Ms. Misako Ueno, and past and present members of my laboratory.

Chapter 7 References

[1] Chambers, E.S., and Vukmanovic, S.M. (2019) Skin barrier immunity and ageing. *Immunology* **160**, 116-125.

[2] Raj, D., Brash, D.E., and Grossman, D. (2006) Keratinocyte apoptosis in epidermal development and disease. *Journal of Investigative Dermatology* **126**, 243-257.

[3] Gaur, M., Dobke, M., and Lunyak, V.V. (2017) Mesenchymal stem cells from adipose tissue in clinical applications for dermatological indications and skin aging. *International Journal of Molecular Science* **18**, 208.

[4] Goleva, E., Berdyshev, E., and Leung, D.Y. (2019) Epithelial barrier repair and prevention of allergy. *Journal of Clinical Investigation* **129**, 1463-1474.

[5] Ogawa, E., Sato, Y., Minagawa, A., and Okuyama, R. (2017) Pathogenesis of psoriasis and development of treatment. *The Journal of Dermatology* **45**, 264-272.

[6] Green, D.R., and Llambi, F. (2015) Cell death signaling. *Cold Spring Harbor Perspectives in Biology* **7**, a006080.

[7] Mariño, G., Niso-Santano, M., Baehrecke, E.H., and Kroemer, G. (2014) Self-consumption: the interplay of autophagy and apoptosis. *Nature Reviews Molecular Cell Biology* **15**, 81–94.

[8] Booth, L.A., Tavallai, S., Hamed, H.A., Cruickshanks, N., and Dent, P. (2014) The role of cell signalling in the crosstalk between autophagy and apoptosis. *Cell Signaling* **26**, 549-555.

[9] Elmore, S. (2007) Apoptosis: a review of programmed cell death. *Toxicologic Pathology* **35**, 495-516.

[10] Mah, L.Y., and Ryan, K.M. (2012) Autophagy and cancer. *Cold Spring Harbor Perspectives in Biology* **4**, a008821.

[11] Martinet, W., Agostinis, P., Vanhoecke, B., Dewaele, M., and De Meyer, G.R. (2009) Autophagy in disease: a double-edged sword with therapeutic potential. *Clinical Science* **116**, 697-712.

[12] Zema, D., Calabrò, P., Folino, A., Tamburino, V., Zappia, G., and Zimbone, S. (2018) Valorisation of citrus processing waste: A review. *Waste Management* **80**, 252-273.

[13] Reham, I.A., Shahira, M.E., Nora, M.A., Mai, F.R., Dalia, M., Amira, H., Dalia, A., Maha, M.S., and Mahitab, H.E.B, (2021) Downregulation of MMP1 expression mediates the anti-aging activity of *Citrus sinensis* peel extract nanoformulation in UV induced photoaging in mice. *Biomedicine & Pharmacotherapy* **138**, 111527.

[14] Anjali, M., Agnieszka, N., Aarti, B., Renata, N.W., and Prince, C, (2021) Characterization of *Citrus nobilis* Peel Methanolic Extract for Antioxidant, Antimicrobial, and Anti-Inflammatory Activity. *Molecules* **26**, 4310.

[15] Nakagawa, H., Takaishi, Y., Tanaka, N., Tsuchiya, K., Shibata, H., and Higuti, T. (2006) Chemical constituents from the peels of *Citrus sudachi*. *Journal of Natural Products* **69**, 1177-1179.

[16] Li, C., and Schluesener, H. (2016) Health-promoting effects of the citrus flavanone hesperidin. *Critical Reviews in Food Science and Nutrition* **57**, 613-631.

[17] Kobayashi, H., Mitani, M., Minatogawa, Y., Hayashi, S., Nakamoto, M., Shuto, E., Nii, Y., and Sakai, T. (2017) Extracts of *Citrus sudachi* peel attenuate body weight gain in C57BL/6 nice fed a high-fat diet. *Journal of Medical Investigation* **64**, 20-23.

[18] Xu, W., Miyamoto, L., Aihara, H., Yamaoka, T., Tanaka, N., Tsuchihashi, Y., Ikeda, Y., Tamaki, T., Kashiwada, Y., and Tsuchiya, K. (2018) Methanol extraction fraction from

Citrus sudachi peel exerts lipid reducing effects in cultured cells. *Journal of Medical Investigation* **65**, 225-230.

[19] Sergeev, I.N., Ho, C.T., Li, Colby, S.J., and Dushenkov, S. (2007) Apoptosis-inducing activity of hydroxylated polymethoxyflavones and polymethoxyflavones from orange peel in human breast cancer cells. *Molecular Nutrition & Food Research* **51**, 1478-1484.

[20] Wang, L., Wang, J., Fang, L., Zheng, Z., Zhi, D., Wang, S., Li, S., Ho, C.T., and Zhao, H. (2014) Anticancer activities of citrus peel polymethoxyflavones related to angiogenesis and others. *BioMed Research International* **2014**, 1-10.

[21] Lai, C.S., Wu, J.C., Ho, C.T., and Pan, M.H. (2015) Disease chemopreventive effects and molecular mechanisms of hydroxylated polymethoxyflavones. *Biofactors* **41**, 301-313.

[22] Zhang, L., Zhang, X., Zhang, C., Bai, X., Zhang, J., Zhao, X., Chen, L., Wang, L., Zhu, C., Cui, L., Chen, R., Zhao, T., and Zhao, Y. (2016) Nobiletin promotes antioxidant and anti-inflammatory responses and elicits protection against ischemic stroke in vivo. *Brain Research* **1636**, 130-141.

[23] Yoshimizu, N., Otani, Y., Saikawa, Y., Kubota, T., Yoshida, M., Furukawa, T., Kumai, K., Kameyama, K., Fujii, M., Yano, M., Sato, T., Ito, A., and Kitajima, M. (2004) Anti-tumour effects of nobiletin, a citrus flavonoid, on gastric cancer include: antiproliferative effects, induction of apoptosis and cell cycle deregulation. *Alimentary Pharmacology & Therapeutics* **20**, 95-101.

[24] Ji, H.Y., Tae, G.L., Kyung, M.L., Ae, J.J., Su, Y.K., and Ki, W.L, (2011) Tangeretin reduces ultraviolet B (UVB)-induced cyclooxygenase-2 expression in mouse epidermal cells by blocking mitogen-activated protein kinase (MAPK) activation and reactive oxygen species (ROS) generation, *Journal of Agricultural and Food Chemistry* **59**, 222-228.

[25] Nakagawa, H., Takaishi, Y., Tanaka, N., Tsuchiya, K., Shibata, H., and Higuti, T. (2006) Chemical constituents from the peels of *Citrus sudachi*. *Journal of Natural Products* **69**, 1177-1179.

[26] Yuasa, K., Tada, K., Harita, G., Fujimoto, T., Tsukayama, M., and Tsuji, A. (2012) Sudachitin, a polymethoxyflavone from Citrus sudachi, suppresses lipopolysaccharide-induced inflammatory responses in mouse macrophage-like RAW264 cells. *Bioscience, Biotechnology, and Biochemistry* **76**, 598-600.

[27] Ohyama, Y., Ito, J., Kitano, V.J., Shimada, J., and Hakeda, Y. (2018) The polymethoxy flavonoid sudachitin suppresses inflammatory bone destruction by directly inhibiting osteoclastogenesis due to reduced ROS production and MAPK activation in osteoclast precursors. *PLoS One*. **13**, e0191192.

[28] Hosokawa, Y., Hosokawa, I., Ozaki, K., and Matsuo, T. (2019) Sudachitin inhibits matrix metalloproteinase-1 and -3 production in tumor necrosis factor-α-stimulated human periodontal ligament cells. *Inflammation* **42**, 1456-1462.

[29] Mitani, M., Minatogawa, Y., Nakamoto, A., Nakamoto, M., Shuto, E., Nii, Y., and Sakai, T. (2019) Sudachitin, polymethoxyflavone from *Citrus sudachi*, enhances antigen-specific cellular and humoral immune responses in BALB/c mice. *Journal of Clinical Biochemistry and Nutrition* **64**, 158-163.

[30] Cursons, J., Gao, J., Hurley, D.G., Print, C.G., Dunbar, P.R., Jacobs, M.D., and Crampin, E.J. (2015) Regulation of ERK-MAPK signaling in human epidermis. *BMC Systems Biology* **9**, 41.

[31] Eckert, R.L., Efimova, T., Dashti, S.R., Balasubramanian, S., Deucher, A., Crish, J.F., Sturniolo, M., and Bone, F. (2002) Keratinocyte Survival, Differentiation, and Death: Many

Roads Lead to Mitogen-Activated Protein Kinase. *Journal of Investigative Dermatology Symposium Proceedings* **7**, 36-40.

[32] Yue, J., and López, J.M. (2020) Understanding MAPK Signaling Pathways in Apoptosis. *International Journal of Molecular Science* **21**, 2346.

[33] Guo, Y., Pan, W., Liu, S., Shen, Z., Xu, Y., and Hu, L. (2020) ERK/MAPK signalling pathway and tumorigenesis (Review). *Experimental and Therapeutic Medicine* **19**, 1997-2007.

[34] Yang, J., Sun, L., Han, J., Zheng, W., and Peng, W. (2019) DUSP1/MKP-1 regulates proliferation and apoptosis in keratinocytes through the ERK/Elk-1/Egr-1 signaling pathway. *Life Sciences* **223**, 47-53.

[35] Schmidt, M., Goebeler, M., Posern, G., Feller, S.M., Seitz, C.S., Bröcker, E.B., Rapp, U.R., and Ludwig, S. (2000) Ras-independent Activation of the Raf/MEK/ERK Pathway upon Calcium-induced Differentiation of Keratinocytes. *Journal of Biological Chemistry* **275**, 41011-41017.

[36] Shi, J., Zeng, X., Zhou, M., and Chen, Q. (2008) Activation of ERK-FAK Signaling Pathway and Enhancement of Cell Migration Involved in the Early Interaction Between Oral Keratinocytes and Candida albicans. *Mycopathologia* **167**, 1-7.

[37] Jia, J., Li, C., Luo, S., Liu, S.F., Yang, J., Wang, X., Wang, N., Lai, B., Lei, T., Wang, Q., Xiao, S., Shao, Y., and Zheng, Y. (2016) Yes-Associated Protein Contributes to the Development of Human Cutaneous Squamous Cell Carcinoma via Activation of RAS. *Journal of Investigative Dermatology* **136**, 1267-1277.

[38] Kim, H.S., Quon, M.J., and Kim, J.A. (2014) New insights into the mechanisms of polyphenols beyond antioxidant properties; lessons from the greentea polyphenol, epigallocatechin 3-gallate. *Redox Biology* **187**, 187-195.

[39] Yao, L.H., Jiang, Y.M., Shi, J., Tomás-Barberán, F.A., Datta, N., Singanusong, R., and Chen, S.S. (2004) Flavonoids in food and their health benefits. *Plant Foods for Human Nutrition* **59**, 113-122.

[40] Hasima, N., and Ozpolat, B. (2014) Regulation of autophagy by polyphenolic compounds as a potential therapeutic strategy for cancer. *Cell Death & Disease* **5**, e1509.

[41] Moon, J.Y., and Cho, S.K. (2016) Nobiletin induces protective autophagy accompanied by ER-stress mediated apoptosis in human gastric cancer SNU-16 cells. *Molecules* **21**, e914.

[42] Tsukayama, M., Sasaki, T., Yamamoto, K., Kawamura, Y., and Ichikawa, R. (2010) Microwave-assisted extraction and methylation of useful flavones from waste peels of *Citrus sudachi*. *Nippon Shokuhin Kagaku Kogaku Kaishi* **57**, 427-433.

[43] Boukamp, P., Petrussevska, R.T., Breitkreutz, D., Hornung, J., Markham, A., and Fusenig N.E. (1988) Normal keratinization in a spontaneously immortalized aneuploid human keratinocyte cell line. *Journal of Cell Biology* **106**, 761-771.

[44] Yuasa, K., Ota, R., Matsuda, S., Isshiki, K., Inoue, M., and Tsuji, A. (2015) Suppression of death-associated protein kinase 2 by interaction with 14-3-3 proteins. *Biochemical and Biophysical Research Communications* **464**, 70-75.

[45] Kabeya, Y., Mizushima, N., Ueno, T., Yamamoto, A., Kirisako, T., Noda, T., Kominami, E., Ohsumi, Y., and Yoshimori, T. (2000) LC3, a mammalian homologue of yeast Apg8p, is localized in autophagosome membranes after processing. *EMBO Journal* **19**, 5720-5728.

[46] Iwashita, H., Sakurai, H.T., Nagahora, N., Ishiyama, M., Shioji, K., Sasamoto, K., Okuma, K., Shimizu, S., and Ueno, Y. (2018) Small fluorescent molecules for monitoring autophagic flux. *FEBS Letter* **59**, 2559-2567.

[47] Wong, V.K., Li, T., Law, B.Y., Ma, E.D., Yip, N.C., Michelangeli, F., Law C.K., Zhang, M.M., Lam, K.Y., Chan, P.L., and Liu, L. (2013) Saikosaponin-d, a novel SERCA inhibitor, induces autophagic cell death in apoptosis-defective cells. *Cell Death & Disease* **4**, e720.

[48] Gao, Z., Gao, W., Zeng, S.L., Li, P., and Liu, E.H. (2018) Chemical structures, bioactivities and molecular mechanisms of citrus polymethoxyflavones. *Journal of Functional Foods* **40**, 498-509.

[49] Akao, Y., Itoh, T., Ohguchi, K., Iinuma, M., and Nozawa, Y. (2008) Interactive effects of polymethoxy flavones from citrus on cell growth inhibition in human neuroblastoma SH-SY5Y cells. *Bioorganic & Medicinal Chemistry* **16**, 2803-2810.

[50] Li, S., Pan, M.H., Lai, C.S., Lo, C.Y., Dushenkov, S., and Ho, C.T. (2007) Isolation and syntheses of polymethoxyflavones and hydroxylated polymethoxyflavones as inhibitors of HL-60 cell lines. *Bioorganic & Medicinal Chemistry* **15**, 3381-3389.

[51] Chen, C., Ono, M., Takeshima, M., and Nakano, S. (2014) Antiproliferative and apoptosis-inducing activity of nobiletin against three subtypes of human breast cancer cell lines. *Anticancer Research* **34**, 1785-1792.

[52] Huang, K., Chen, Y., Zhang, R., Wu, Y., Ma, Y., Fang, X., and Shen, S. (2018) Honokiol induces apoptosis and autophagy via the ROS/ERK1/2 signaling pathway in human osteosarcoma cells in vitro and in vivo. *Cell Death & Disease* **9**, 157.

[53] Xie, J., Yun, J.P., Yang, Y.N., Hua, F., Zhang, X.W., Lin, H., Lv, X.X., Li, K., Zhang, P.C., and Hu, Z.W. (2017) A novel ECG analog 4-(S)-(2,4,6-trimethylthiobenzyl)-epigallocatechin gallate selectively induces apoptosis of B16-F10 melanoma via activation of autophagy and ROS. *Scientific Reports* **7**, 42194.

[54] Cao, C., Liu, B., Zeng, C., Lu, Y., Chen, S., Yang, L., Li, B., Li, Y., and Li, Y. (2014) A polymethoxyflavone from Laggera pterodonta induces apoptosis in imatinib-resistant

K562R cells via activation of the intrinsic apoptosis pathway. *Cancer Cell International* **14**, 137.

[55] Charoensinphon, N., Qiu, P., Dong, P., Zheng, J., Ngauv, P., Cao, Y., Li, S., Ho, C.T., and Xiao, H. (2013) 5-demethyltangeretin inhibits human nonsmall cell lung cancer cell growth by inducing G2/M cell cycle arrest and apoptosis. *Molecular Nutrition & Food Research* **57**, 2103-2111.

[56] Zhu, G.H., Dai, H.P., Shen, Q., Ji, O., Zhang, Q., and Zhai, Y.L. (2016) Curcumin induces apoptosis and suppresses invasion through MAPK and MMP signaling in human monocytic leukemia SHI-1 cells. *Pharmaceutical Biology* **54**, 1303-1311.

[57] Wu, X.P., Xiong, M., Xu, C.S., Duan, L.N., Dong, Y.Q., Luo, Y., Niu, T.H., and Lu, C.R. (2015) Resveratrol induces apoptosis of human chronic myelogenous leukemia cells in vitro through p38 and JNK-regulated H2AX phosphorylation. *Acta Pharmacologica Sinica* **36**, 353-361.

[58] Sui, X., Kong, N., Ye, L., Han, W., Zhou, J., Zhang, Q., He, C., and Pan, H. (2014) p38 and JNK MAPK pathways control the balance of apoptosis and autophagy in response to chemotherapeutic agents. *Cancer Letter* **344**, 174-179.

[59] Peus, D., Vasa, R.A., Meves, A., Beyerle, A., and Pittelkow, M.R. (2000) UVB-induced epidermal growth factor receptor phosphorylation is critical for downstream signaling and keratinocyte survival. *Photochemistry and Photobiology* **72**, 135-140.

[60] Takahashi, H., Ibe, M., Nakamura, S., Ishida, Y.A., Hashimoto, Y., and Iizuka, H. (2002) Extracellular regulated kinase and c-Jun N-terminal kinase are activated in psoriatic involved epidermis. *Journal of Dermatological Science* **30**, 94-99.

[61] Kamemura, N., Murakami, S., Komatsu, H., Sawanoi, M., Miyamoto, K., Ishidoh, K., Kishimoto, K., Tsuji, A., and Yuasa, K. (2017) Type II cGMP-dependent protein kinase

negatively regulates fibroblast growth factor signaling by phosphorylating Raf-1 at serine 43 in rat chondrosarcoma cells. *Biochemical and Biophysical Research Communications* **483**, 82-87.

[62] Koivisto, L., Jiang, G., Häkkinen, L., Chan, B., and Larjava, H. (2006) HaCaT keratinocyte migration is dependent on epidermal growth factor receptor signaling and glycogen synthase kinase-3α. *Experimental Cell Research* **312**, 2791-2805.

[63] Liang, P., Jiang, B., Yang, X., Xiao, X., Huang, X., Long, J., Zhang, P., Zhang, M., Xiao, M., Xie, T., and Huang, X. (2008) The role of peroxisome proliferator-activated receptor-β/δ in epidermal growth factor-induced HaCaT cell proliferation. *Experimental Cell Research* **314**, 3142-3151.

[64] Kimura, J., Nemoto, K., Yokosuka, A., Mimaki, Y., Degawa, M., and Ohizumi, Y. (2013) 6-demethoxynobiletin, a nobiletin-analog citrus flavonoid, enhances extracellular signal-regulated kinase phosphorylation in PC12D cells. *Biological and Pharmaceutical Bulletin* **36**, 1646-1649.

[65] Cheng, H.L., Hsieh, M.J., Yang, J.S., Lin, C.W., Lue, K.H., Lu, K.H., and Yang, S.F. (2016) Nobiletin inhibits human osteosarcoma cells metastasis by blocking ERK and JNK-mediated MMPs expression. *Oncotarget* **7**, 35208-35223.

[66] Tse, W.P., Che, C.T., Liu, K., and Lin, Z.X. (2006) Evaluation of the anti-proliferative properties of selected psoriasis-treating Chinese medicines on cultured HaCaT cells. *Journal of Ethnopharmacology* **108**, 133-141.

[67] Gargalionis, A.N., Malakou, L.S., Adamopoulos, C., Piperi, C., Theohari, I., Nokhbehsaim, M., Deschner, J., Kokkalis, G., Korkolopoulou, P., Papadavid, E., Papavassiliou, A.G., and Basdra, E.K. (2018) Polycystin-1 downregulation induces ERK-dependent mTOR pathway

activation in a cellular model of psoriasis. *Biochimica et Biophysica Acta - Molecular Basis of Disease* **1864**, 3468-3476.

[68] Ding, W., Cao, Y., Xing, F., Tao, M., Fu, H., Luo, H., and Yang, X. (2019) A preliminary study of the effect of semaphorin 3A and acitretin on the proliferation, migration, and apoptosis of HaCaT cells. *Indian Journal of Dermatology* **64**, 250.

[69] Huang, T.H., Lin, C.F., Alalaiwe, A., Yang, S.C., and Fang, J.Y. (2019) Apoptotic or antiproliferative activity of natural products against keratinocytes for the treatment of psoriasis. *International Journal of Molecular Science* **20**, 2558.

[70] Wang, S., Zhang, Z., Peng, H., and Zeng, K. (2019) Recent advances on the roles of epidermal growth factor receptor in psoriasis. *American Journal of Translational Research* **11**, 520-528.

[71] Flisiak, I., Szterling, J.M., Baran, A., and Rogalska, T. M. (2014) Effect of psoriasis activity on epidermal growth factor (EGF) and the concentration of soluble EGF receptor in serum and plaque scales. *Clinical and Experimental Dermatology* **39**, 461-467.

[72] Wee, P., and Wang, Z. (2017) Epidermal Growth Factor Receptor Cell Proliferation Signaling Pathways. *Cancers* **9**, 52.

[73] Waltenberger, B., Avula, B., Ganzera, M., Khan, I., Stuppner, H., and Khan, S. (2008) Transport of sennosides and sennidines from Cassia angustifolia and Cassia senna across Caco-2 monolayers—An in vitro model for intestinal absorption. *Phytomedicine* **15**, 373-377.

[74] Zhang, C., Xu, Q., Tan, X., Meng, L., Wei, G., Liu, Y., and Zhang, C. (2017) Astilbin decreases proliferation and improves differentiation in HaCaT keratinocytes. *Biomedicine & Pharmacotherapy* **93**, 713-720.

[75] Deyrieux, A.F., and Wilson, V.G. (2007) In vitro culture conditions to study keratinocyte differentiation using the HaCaT cell line. *Cytotechnology* **54**, 77-83.

[76] Shebaby, W.N., Mroueh, M.A., Boukamp, P., Taleb, R.I., Bodman, S.K., Sibai, M.E., and Daher, C.F. (2017) Wild carrot pentane-based fractions suppress proliferation of human HaCaT keratinocytes and protect against chemically-induced skin cancer. *BMC Complementary Medicine and Therapies* **17**, 1-14.

[77] Singkhorn, S., Tantisira, M.H., Tanasawet, S., Hutamekalin, P., Wongtawatchai, T., and Sukketsiri, W. (2018) Induction of keratinocyte migration by ECa 233 is mediated through FAK/Akt, ERK, and p38 MAPK signaling. *Phytotherapy Research* **32**, 1397-1403.

[78] Yamaoka, T., Ohba, M., and Ohmori, T. (2017) Molecular-Targeted Therapies for Epidermal Growth Factor Receptor and Its Resistance Mechanisms. *International Journal of Molecular Science* **18**, 2420.

[79] Adachi, S., Nagao, T., Ingólfsson, H.I., Maxfield, F.R., Andersen, O.S., Kopelovich, L., and Weinstein, I.B. (2007) The Inhibitory Effect of (-)-Epigallocatechin Gallate on Activation of the Epidermal Growth Factor Receptor Is Associated with Altered Lipid Order in HT29 Colon Cancer Cells. *Cancer Research* **67**, 6493-6501.

[80] Ziv, E., Rotem, C., Miodovnik, M., Ravid, A., and Koren, R. (2008) Two modes of ERK activation by TNF in keratinocytes: Different cellular outcomes and bi-directional modulation by vitamin D. *Journal of Cellular Biochemistry* **104**, 606-619.

[81] Nishimura, M., Shin, M.S., Singhirunnusorn, P., Suzuki, S., Kawanishi, M., Koizumi, K., Saiki, I., and Sakurai, H. (2009) TAK1-Mediated Serine/Threonine Phosphorylation of Epidermal Growth Factor Receptor via p38/Extracellular Signal-Regulated Kinase: NF-κB-Independent Survival Pathways in Tumor Necrosis Factor Alpha Signaling. *Molecular and Cellular Biology* **29**, 5529-5539.

[82] Sabio, G., and Davis, R.J. (2014) TNF and MAP kinase signalling pathways. *Seminars in Immunology* **26**, 237-245.

[83] Karoulia, Z., Gavathiotis, E., and Poulikakos, P.I. (2017) New perspectives for targeting RAF kinase in human cancer. *Nature Reviews Cancer* **17**, 676-691.

[84] Lee, S.E., and Lee, S.H. (2018) Skin Barrier and Calcium. *Annals of Dermatology* **30**, 265-275.

[85] Lacouture, M.E. (2006) Mechanisms of cutaneous toxicities to EGFR inhibitors. *Nature Reviews Cancer* **6**, 803-812.

[86] Kolev, V., Mandinova, A., Viniegra, J.G., Hu, B., Lefort, K., Lambertini, C., Neel, V., Dummer, R., Wagner, E.F., and Dotto, G.P. (2008) EGFR signalling as a negative regulator of Notch1 gene transcription and function in proliferating keratinocytes and cancer. *Nature Cell Biology* **10**, 902-911.

[87] Seppänen S.P., Karvinen, S., Törrönen, K., Hyttinen, J.M., Jokela, T., Lammi, M.J., Tammi, M.I., andTammi, R. (2003) EGF Upregulates, Whereas TGF-β Downregulates, the Hyaluronan Synthases Has2 and Has3 in Organotypic Keratinocyte Cultures: Correlations with Epidermal Proliferation and Differentiation. *Journal of Investigative Dermatology* **120**, 1038-1044.

[88] Harmon, R.M., Simpson, C.L., Johnson, J.L., Koetsier, J.L., Dubash, A.D., Najor, N.A., Sarig, O., Sprecher, E., and Green, K.J. (2013) Desmoglein-1/Erbin interaction suppresses ERK activation to support epidermal differentiation. *Journal of Clinical Investigation* **123**, 1556-1570.

[89] Commandeur, S., van Drongelen, V., de Gruijl, F.R., and el Ghalbzouri, A. (2012) Epidermal growth factor receptor activation and inhibition in 3D in vitro models of normal skin and human cutaneous squamous cell carcinoma. *Cancer Science* **103**, 2120-2126.

[90] Uribe, P., and Gonzalez, S. (2011) Epidermal growth factor receptor (EGFR) and squamous cell carcinoma of the skin: Molecular bases for EGFR-targeted therapy. *Pathology - Research and Practice* **207**, 337-342.

[91] Li, L., Li, M., Xu, S., Bu, W., Zhang, M., Gu, H., and Chen, X. (2018) Is Ras a potential target in treatment against cutaneous squamous cell carcinoma? *Journal of Cancer* **9**, 3373-3381.

[92] Su, F., Viros, A., Milagre, C., Trunzer, K., Bollag, G., Spleiss, O., Reis-Filho, J.S., Kong, X., Koya, R.C., Flaherty, K.T., Chapman, P.B., Kim, M.J., Hayward, R., Martin, M., Yang, H., Wang, Q., Hilton, H., Hang, J.S., Noe, J., Lambros, M., Geyer, F., Dhomen, N., Duvaz, I.N., Zambon, A., Duvaz, D.N., Preece, N., Robert, L., Otte, N.J., Mok, S., Kee, D., Ma, Y., Zhang, C., Habets, G., Burton, E.A., Wong, B., Nguyen, H., Kockx, M., Andries, L., Lestini, B., Nolop, K.B., Lee, R.J., Joe, A.K., Troy, J.L., et al. (2012) RAS mutations in cutaneous squamous-cell carcinomas in patients treated with BRAF inhibitors. *The New England Journal of Medicine* **366**, 207-215.

[93] Li, X., Xie, X., Zhang, L., Meng, Y., Li, N., Wang, M., Zhai, C., Liu, Z., Di, T., Zhang, L., and Li, P. (2019) Hesperidin inhibits keratinocyte proliferation and imiquimod-induced psoriasis-like dermatitis via the IRS-1/ERK1/2 pathway. *Life Sciences* **219**, 311-321.

[94] Nie, Y.C., Wu, H., Li, P.B., Xie, L.M., Luo, Y.L., Shen, J.G., and Su, W.W. (2012) Naringin attenuates EGF-induced MUC5AC secretion in A549 cells by suppressing the cooperative activities of MAPKs-AP-1 and IKKs-IκB-NF-κB signaling pathways. *European Journal of Pharmacology* **690**, 207-213.

[95] Kim, G.D. (2014) Hesperetin Inhibits Vascular Formation by Suppressing of the PI3K/AKT, ERK, and p38 MAPK Signaling Pathways. *Preventive Nutrition and Food Science* **19**, 299-306.

[96] Chen, M., Gu, H., Ye, Y., Lin, B., Sun, L., Deng, W., Zhang, J., and Liu, J. (2010) Protective effects of hesperidin against oxidative stress of tert-butyl hydroperoxide in human hepatocytes. *Food and Chemical Toxicology* **48**, 2980-2987.

[97] Kim, N.I., Lee, S.J., Lee, S.B., Park, K., Kim, W.J., and Moon, S.K. (2008) Requirement for Ras/Raf/ERK pathway in naringin-induced G1-cell-cycle arrest via p21WAF1 expression. *Carcinogenesis* **29**, 1701-1709.

[98] Huang, Y.C., Liu, K.C., and Chiou, Y.L. (2012) Melanogenesis of murine melanoma cells induced by hesperetin, a Citrus hydrolysate-derived flavonoid. *Food and Chemical Toxicology* **50**, 653-659 .

[99] Slambrouck, S.V., Parmar, V.S., Sharma, S.K., de Bondt, B., Foré, F., Coopman, P., Vanhoecke, B.W., Boterberg, T., Depypere, H.T., Leclercq, G., and Bracke, M.E. (2005) Tangeretin inhibits extracellular-signal-regulated kinase (ERK) phosphorylation. *FEBS Letter* **579**, 1665-1669.

[100] Lin, C.W., Hou, W.C., Shen, S.C., Juan, S.H., Ko, C.H., Wang, L.M., and Chen, Y.C. (2008) Quercetin inhibition of tumor invasion via suppressing PKC /ERK/AP-1-dependent matrix metalloproteinase-9 activation in breast carcinoma cells. *Carcinogenesis* **29**, 1807-1815.

Appendix

List of publications

(Main dissertations)

Abe, S. and Yuasa, K.

Sudachitin, a polymethoxyflavone from *Citrus sudachi*, induces apoptosis via the regulation of MAPK pathways in human keratinocyte HaCaT cells

Biochem. Biophys. Res. Commun. **519** (2019) 344-350

Abe, S., Ueno, M., Nishitani, M., Akamatsu, T., Sato, T., Shimoda, M., Kanaoka, H., Nii, Y., Yamasaki, H., and Yuasa, K.

Citrus sudachi peel extract suppresses cell proliferation and promotes the differentiation of keratinocytes through inhibition of the EGFR-ERK signaling pathway

Biomolecules **10** (2020) 1468

(Sub dissertation)

Abe, S., Hirose, S., Nishitani, M., Yoshida, I., Tsukayama, M., Tsuji, A., and Yuasa, K.

Citrus peel polymethoxyflavones, sudachitin and nobiletin, induce distinct cellular responses in human keratinocyte HaCaT cells

Biosci. Biotechnol. Biochem. **82** (2018) 2064-2071